

Receptor activity modifying protein-directed G protein signaling specificity for the calcitonin gene-related peptide family of receptors

Cathryn Weston^{1*}, Ian Winfield^{1,2*}, Matthew Harris², Rose Hodgson¹, Archana Shah¹, Simon J. Dowell³, Juan Carlos Mobarec⁴, David A Woodlock⁴, Christopher A Reynolds⁴, David R. Poyner⁵, Harriet A. Watkins⁶ and Graham Ladds^{2#}

¹ Division of Biomedical Cell Biology, Warwick Medical School, University of Warwick, Coventry, CV4 7AL, UK.

² Department of Pharmacology, University of Cambridge, Tennis Court Road, Cambridge, CB2 1PD, UK.

³ Department of Platform Technology and Science, GlaxoSmithkline, Hertfordshire, SG1 2NY, UK.

⁴ School of Biological Sciences, University of Essex, Wivenhoe Park, Colchester, Essex, CO4 3SQ, UK.

⁵ School of Life and Health Sciences, Aston University, Aston Triangle, Birmingham, B4 7ET, UK.

⁶ School of Biological Sciences, University of Auckland, Auckland, New Zealand and Maurice Wilkins Centre for Molecular Biodiscovery, University of Auckland, Auckland, New Zealand.

Running Title: G protein bias in CLR-based receptors.

* I.W. and C.W. contributed equally to the work.

To whom correspondence should be addressed: Dr Graham Ladds, Department of Pharmacology, University of Cambridge, Tennis Court Road, Cambridge, CB2 1PD Tel; +44 (0) 1223 334020. E-mail: grl30@cam.ac.uk.

Keywords: CGRP, Adrenomedullin, Adrenomedullin 2, G protein-coupled receptors (GPCRs), receptor activity modifying proteins (RAMPs), signal bias, signal transduction, yeast, molecular modelling, molecular dynamics.

Abstract

The calcitonin gene-related peptide (CGRP) family of G protein-coupled receptors (GPCRs) is formed through association of the calcitonin receptor-like receptor (CLR) and one of three receptor activity-modifying proteins (RAMPs). Binding of one of the three peptide ligands, CGRP, adrenomedullin (AM) or intermedin/adrenomedullin2 (AM2) is well known to result in a $G\alpha_s$ -mediated increase in cAMP. Here we use modified yeast strains that couple receptor activation to cell growth, via chimeric yeast/ $G\alpha$ subunits, and HEK-293 cells to characterize the effect of different RAMP and ligand combinations on this pathway. We not only demonstrate functional couplings to both $G\alpha_s$ and $G\alpha_q$ but also identify a $G\alpha_i$ component to CLR signaling in both yeast and HEK-293 cells, which is absent in HEK-293S cells. We show that the CGRP family of receptors displays both ligand and RAMP-dependent signaling bias between $G\alpha_s$, $G\alpha_i$ and $G\alpha_{q/11}$ pathways. The results are discussed in the context of RAMP interactions probed through molecular modelling and molecular dynamics simulations of the RAMP-GPCR-G protein complexes. This study further highlights the importance of RAMPs to CLR pharmacology, and to bias in general, as well as identifying the importance of choosing an appropriate model system for the study of GPCR pharmacology.

modulation of vascular tone (4-6). AM2 affects the vascular system in a similar manner to AM (7-9). Like CGRP, AM and AM2 are also cardioprotective and their administration results in decreased blood pressure and increased speed of recovery from myocardial infarction (10-11).

CGRP, AM and AM2 activate three receptors which share a common class B G protein-coupled receptor (GPCR) subunit, the calcitonin receptor-like receptor (CLR) (12). In each receptor CLR forms a heterodimer with receptor activity-modifying proteins (RAMPs) 1, 2 or 3. The formation of this heterodimer is obligatory for receptor function and efficient translocation of both subunits to the cell surface (13). Heterodimerisation with RAMP 1, 2 or 3 forms the CGRP, AM₁ or AM₂ receptors respectively (13). The peptide ligands activate each receptor with differing potencies (1, 12).

Activation of all three CLR-based receptors by CGRP, AM or AM2 generates increased cAMP production through coupling to the stimulatory G protein, $G\alpha_s$ (1, 12, 14). However, CGRP, AM and AM2 can signal through other pathways (1, 15-16). Several studies have indicated that the CGRP family of receptors can also couple to $G\alpha_{i/o}$ subunits, since their cAMP responses can be significantly increased through treatment with pertussis toxin (PTX), particularly in electrically excitable cells (17-20). The AM/AM₂ receptor cAMP signaling in HEK-293 cells has also been shown to be PTX sensitive (21). The existing information on stimulation of signaling by CGRP, AM or AM2 other than through the $G\alpha_s$ -cAMP pathway has been predominantly gained from physiological studies and the relative signaling bias of CGRP, AM and AM2 at the three CLR-based receptors, even for the cAMP pathway, remains to be determined.

The study of signaling bias *in vivo* is complicated by crosstalk from the wide range of signaling pathways present in certain cell lines or primary cell cultures. The *Saccharomyces cerevisiae* growth system (22) provides a robust assay to enable the examination of the coupling of a GPCR of choice to single G protein subunits. This is achieved through replacing the last 5 amino acids of the native yeast G

Introduction

Calcitonin gene-related peptide (CGRP), adrenomedullin (AM) and adrenomedullin 2 (AM2, also known as intermedin) are members of the calcitonin peptide family (1). This family also includes calcitonin and amylin. CGRP is an extremely abundant neuropeptide, widely distributed throughout the sensory nervous system. It is a very potent vasodilator, released during neurogenic inflammation and is particularly implicated in the onset of migraine. It is also cardioprotective and is associated with both pro- and anti-inflammatory actions (2-3). AM is produced by the vascular endothelium and has extensive effects on the cardiovascular system including stimulation of angiogenesis and the

protein with the corresponding sequence from the human G protein of choice. (22-23). This assay has recently been successfully employed to characterize the signaling pathways underlying the glucagon-like peptide 1 (GLP-1) receptor response to GLP-1 and the many receptor agonist mimetics available (24-25). Miret and co-workers in 2002, very elegantly described the functional expression of the CLR with RAMP1 and RAMP2 in yeast (26). However, somewhat surprisingly, given the more recent interest in signaling bias, further characterization of RAMP-CLR combinations in yeast has not been performed.

In this study we have utilized *S. cerevisiae* to express either RAMP1, 2 or 3 along with CLR in order to assess the coupling of the three CGRP family receptors to different human $G\alpha$ subunits upon stimulation with either CGRP, AM or AM2. We demonstrate that all members of the CGRP receptor family successfully couple to GPA1/ $G\alpha_s$, GPA1/ $G\alpha_i$ and GPA1/ $G\alpha_q$ yeast chimeras and that the coupling preference of each receptor is dependent upon the stimulating ligand. The results obtained from the yeast system were verified in HEK-293 mammalian cell lines by the assessment of cAMP accumulation (which showed sensitivity to PTX) and mobilizations of intracellular calcium ($i(Ca^{2+})$). The data confirm that RAMPs alter the ability of each peptide to couple to G proteins; it also indicates that the G proteins influence the rank order of agonist potency at the different receptors. For CGRP, AM and AM2 this means that potent activation of what would not generally be considered their 'normal' receptors can be observed when alternative downstream pathways, such as stimulation of $G\alpha_i$, or mobilizations of $i(Ca^{2+})$ are considered.

Considerable understanding has been gained into class B GPCR structure, function and dynamics (27), primarily through molecular dynamic simulations (28-32). Consequently, in order to gain insight into possible mechanisms behind our experimental results, we have used molecular modelling and molecular dynamics simulations of RAMP complexes with CLR and the glucagon receptor (GCGR) to suggest a mechanism whereby the C-terminal tail of the RAMPs may influence G protein bias at the CLR. Finally we demonstrate that care is required when selecting an appropriate mammalian cell line to use when investigating G protein-bias since analysis of a HEK-293S cell line failed to show any $G\alpha_i$ -coupling for any of the RAMP-CLR complexes thus highlighting that agonist bias can be directly influenced by the cellular background.

Results

G α_s coupling of CLR-based receptors - We co-expressed CLR under the control of the strong PGK promoter, with RAMP1, RAMP2 or RAMP3 independently in a yeast strain containing a chimeric $G\alpha$ -subunit in which the C-terminal 5 amino acids of GPA1 had been replaced with those of mammalian $G\alpha_s$, in order to study the coupling of the resultant receptors to a system expressing just a single G protein. Concentration-response curves were constructed for growth of *S. cerevisiae* for each RAMP-CLR combination (i.e. the CGRP, AM₁ and AM₂ receptors) using the agonists CGRP, AM and AM2. When CLR was co-expressed with RAMP1 all three ligands appeared to generate an equivalent level of response but with differing potencies (Figure 1A; Table 1). This generates a rank order of potency for the three ligands of CGRP > AM > AM2. Application

of the operational model of pharmacological agonism (34) indicates that all three ligands exhibit similar efficacies ($\log \tau$) in yeast when CLR and RAMP1 are co-expressed (Figure 1D; Table 1). RAMP2 co-expression with CLR generated a functional receptor (Figure 1B) with rank ligand potencies of AM > AM2 = CGRP. AM2 appeared to behave as a partial agonist with a reduced $\log \tau$ at the RAMP2-CLR heterodimer when compared to the other peptide agonists (Table 1). AM had a significantly higher efficacy ($p < 0.05$) than that displayed by CGRP. Expression of RAMP3 with CLR in *S. cerevisiae* generated a functional receptor where all three ligands activated GPA1/ $G\alpha_s$ coupled signaling with similar potencies and efficacies (Figure 1C).

We sought to confirm the pharmacology observed in the *S. cerevisiae* growth assay of the RAMP-CLR complexes in mammalian cell lines. For this we have used HEK-293 cells that do not functionally express any RAMPs (25). Co-transfection of CLR and RAMP1 generated a rank order of ligand potency of CGRP >> AM = AM2. The rank order of ligand potency with co-transfection of CLR and RAMP2 was AM > CGRP >> AM2 and for CLR and RAMP3 was AM2 = AM > CGRP (Figure 2, Table 2). It is worth noting that, in our HEK-293 cells, only AM acts as a full agonist against the CLR when in complex with either RAMP2 or RAMP3. Overall the mammalian and yeast data show similar results with the most potent ligand at each receptor remaining the same in each case.

G α_i coupling of CLR-based receptors - To address the possibility that the CGRP family of receptors may couple not only to $G\alpha_s$ but also to other subunits we returned to the *S. cerevisiae* growth assay. In this case the yeast strain used contained a chimeric GPA1/ $G\alpha$ subunit including the last 5 residues of mammalian $G\alpha_i$. We once again constructed concentration-response curves for yeast growth to the three agonists, CGRP, AM and AM2. The co-expression of CLR and RAMP1 resulted in similar potencies for CGRP, AM and AM2, (Table 1) however, AM and AM2 displayed significantly increased efficacies relative to CGRP for activation of GPA1/ $G\alpha_i$ (Table 1; Figure 3A and D). In contrast, when RAMP2 and CLR are co-transformed into the GPA1/ $G\alpha_i$ yeast strain the rank order of ligand potency for GPA1/ $G\alpha_i$ yeast-based growth was CGRP > AM = AM2 (Table 1, Figure 3B). AM2 showed a significantly decreased efficacy compared with the other peptides (Table 1, Figure 3D). Similarly to the RAMP1-CLR heterodimer, the combination of CLR and RAMP3 expressed in the GPA1/ $G\alpha_i$ strain resulted in similar potencies for CGRP, AM and AM2 (Table 1, Figure 3C). However, AM2 displayed a significantly reduced efficacy when compared to AM (Table 1, Figure 3D).

In mammalian cells the $G\alpha_s$ and $G\alpha_i$ subunits act in opposition to regulate cAMP production. Therefore if a receptor can couple to both subunits in mammalian cells, the cAMP response measured is the result of a combination of the contribution from both pathways. Treatment of cells with PTX has been shown to uncouple receptors from the $G\alpha_i$ subunit and therefore remove any inhibition of cAMP production. We sought to confirm the apparent $G\alpha_s$ - $G\alpha_i$ coupling bias exhibited by the different RAMP-CLR combinations in the yeast reporter strains by measuring cAMP production from transiently transfected mammalian cells following PTX treatment.

Pre-treatment of HEK-293 cells co-expressing RAMP1 with the CLR resulted in little overall increases in CGRP-mediated cAMP production (Figure 4A). However, a significant elevation in E_{\max} was observed in the same PTX-treated, RAMP1-CLR expressing cells, when challenged with either AM or AM2 (Figure 4, Table 3) suggesting that a $G\alpha_i$ component for both these ligands had been removed (Table 3). HEK-293 cells expressing CLR with either RAMP2 (Figure 4B) or RAMP3 (Figure 4C) displayed PTX-induced increases in E_{\max} for cAMP accumulation, following stimulation with both CGRP and AM2 (Table 3). However, for both combinations, the AM response appeared to be unaffected by PTX treatment, suggesting that little $G\alpha_i$ coupling was present. Indeed, it is worth noting, that the cognate ligand for each receptor (CGRP for RAMP1-CLR and AM for RAMP2-CLR or RAMP3-CLR) did not appear to display an increased E_{\max} upon PTX-treatment, suggesting limited $G\alpha_i$ components in these cases. Importantly, PTX treatment of un-transfected HEK-293 cells did not result in a change in overall levels of cAMP accumulation as determined by forskolin stimulation (untreated = 16.57 ± 2.5 pmol cell⁻¹; treated = 16.45 ± 2.4 pmol cell⁻¹) thereby confirming that the effects observed were specific to the RAMP-CLR combinations. Thus, there is abundant evidence that receptor and ligands can activate $G\alpha_i$ in a mammalian cell, albeit in a complex pattern.

Cell line variability in G protein expression - The HEK-293 human cell lineage has undergone a number of modifications (35). One such lineage, HEK-293S was adapted for growth in suspension (36). Interestingly, HEK-293S lines have also been reported to lack expression of RAMPs and therefore provide an alternative background for investigating the modulation of GPCR signal transduction (37, 38). Given that previous reports have suggested that some of the effects observed with RAMPs are cell-type dependent (37, 39), we utilized HEK-293S cells as an alternative cell line. Surprisingly, and in contrast to that observed for HEK-293 cells, HEK-293S cells pre-treated with PTX and co-expressing either RAMP1, RAMP2 or RAMP3 with CLR failed to demonstrate any significant change in either potency or E_{\max} when challenged with CGRP, AM or AM2 (Figure 5 A-C and Table 4; compare with Figure 4 A-C). These results suggest that in HEK-293S cells, the RAMP-CLR combinations display little $G\alpha_i$ -mediated responses. This led us to speculate about the respective G protein content for the two cell lines. Using semi-quantitative RT-PCR we assessed the expression of twelve $G\alpha$ subunits (Figure 6 A and B) in both mammalian cell lines. In the HEK-293 cells we were able to detect the expression of 10 $G\alpha$ subunits, with a profile similar to that previously documented for these cells (40). Transcripts were not detectable for $G\alpha_{14}$ or $G\alpha_{15}$ subunits. Interestingly, in comparison to the HEK-293 cells, the HEK-293S cells displayed significantly lower expression of two $G\alpha_i$ subunits (relative to GAPDH) but broadly similar levels of all others $G\alpha$ subunits. Furthermore, there was a much better correlation between the pEC₅₀ values for the ligands on HEK-293 and HEK-293S cells when the former had been pretreated with PTX, to remove the $G\alpha_i$ component, suggesting that the differences in $G\alpha_i$ expression between the two cell lines does have functional significance (Figure 6C, $r = 0.80$ (95% confidence interval 0.27 to 0.96) with PTX v 0.52 (95% confidence interval -0.22 to 0.89) without PTX; $p < 0.05$). Importantly, this data

demonstrates the need for caution when choosing cells for assessing G protein-mediated signaling responses.

G $\alpha_{q/11}$ coupling of CLR-based receptors - To provide a complete investigation of the G protein coupling of the RAMP-CLR complexes we extended our study to include the remaining 9 GPA1/ $G\alpha$ yeast chimera-expressing strains. Coupling with the RAMP-CLR heterodimers was only observed in one additional strain that representing $G\alpha_q$ (strain MMY89). Concentration-response curves were generated (Figure 7 A-C, Table 1), demonstrating at RAMP1-CLR all three ligands displayed similar potencies, with CGRP being the most efficacious (log τ , Table 1), as expected for the cognate ligand at this receptor. AM2 is the most potent ligand when activating the RAMP2-CLR complex, whilst having a reduced E_{\max} and log τ , relative to CGRP and AM (Table 1). With RAMP3-CLR a rank order of ligand potency of AM>AM2>CGRP was observed (Figure 7C, Table 1), with all three ligands displaying broadly similar efficacies (Table 1).

Ligand-engendered G protein bias - To provide a means by which to determine the relative bias each agonist displays at each RAMP-CLR complex for the three different chimeric G proteins (in yeast) we calculated the bias factor (expressed as $\Delta\Delta(\tau/Ka)$) (41). For the RAMP1-CLR heterodimer values were calculated relative to CGRP, whereas when CLR was expressed with RAMP2 or RAMP3 the reference ligand was AM. In all cases the reference pathway used was GPA1/ $G\alpha_s$ (Figure 7E). The bias plots demonstrated that at the RAMP1-CLR complex AM2 shows a much greater bias towards signaling via GPA1/ $G\alpha_i$ and GPA1/ $G\alpha_q$, relative to CGRP, whilst AM shows a bias profile approximately equal to CGRP. With RAMP2-CLR however, CGRP shows a much greater bias towards GPA1/ $G\alpha_i$ signaling over GPA1/ $G\alpha_s$ and GPA1/ $G\alpha_q$, whilst AM2 is more biased towards GPA1/ $G\alpha_q$. In the presence of RAMP3 all three ligands are equally biased towards GPA1/ $G\alpha_s$ and GPA1/ $G\alpha_i$, but CGRP and AM are less biased towards GPA1/ $G\alpha_q$ signaling, relative to AM2.

Activation of RAMP-CLR complexes leads to mobilization of intracellular Ca²⁺ in mammalian cells - In order to confirm our findings from *S. cerevisiae* we again utilized HEK 293 cells transiently expressing the CLR in conjunction with each RAMP, and measured release of i(Ca²⁺) upon stimulation with CGRP, AM and AM2. Whilst all three ligands resulted in calcium mobilization at each RAMP-CLR complex (Figure 8, Table 5), these results differed slightly from that observed in *S. cerevisiae*. At both RAMP1 and RAMP2-CLR a rank order of ligand potency of CGRP=AM>AM2 was seen, whilst CGRP was the most efficacious ligand (Table 5). With RAMP3-CLR both AM and AM2 were equipotent, with CGRP being the least potent agonist. Treatment with PTX was seen to have no effect upon the levels of calcium released in response to the three ligands, at any RAMP:CLR complex.

To confirm our yeast findings that the CLR can couple to $G\alpha_q$ and thereby promote i(Ca²⁺) mobilization in mammalian cells, we utilized the known selective $G\alpha_{q/11}$ inhibitor YM-254890 (42). Pre-treatment with YM-254890 for 30 min prior to stimulation with AM and AM2 was sufficient to abolish all i(Ca²⁺) mobilization at all RAMP-CLR complexes. Furthermore responses to CGRP at all 3 RAMP-CLR complexes was also considerably attenuated with i(Ca²⁺) release only being detected when cells were stimulated with CGRP in the

micromolar range. Similar data was obtained using HEK 293S cells (Table 5) suggesting that despite differences in $G\alpha_i$ content, release of $i(\text{Ca}^{2+})$ is consistent between the 2 cell types. These findings suggest that all three ligands are able to initiate calcium mobilization at all three RAMP-CLR complexes in a $G\alpha_q$ -dependent manner, in both mammalian cell lines.

Pathway bias at the RAMP-CLR complexes – Through calculating the change in the ratio of $\log(\tau/Ka)$ between cAMP accumulation and release of $i(\text{Ca}^{2+})$, it is possible to determine the extent of signaling bias for a ligand (Figure 9 A). In HEK-293 cells all ligands show cAMP bias over $i(\text{Ca}^{2+})$, except for AM2 and CGRP at RAMP2-CLR and RAMP3-CLR, respectively. In contrast, in HEK-293S cells all ligands show clear bias towards cAMP at each RAMP-CLR complex. Interestingly, treatment of HEK-293 cells with PTX, generates bias profiles similar to that observed for HEK-293S cells (Figure 9).

Further analysis of these bias factors, relative to the cognate ligand at each RAMP-CLR complex (Figure 9 B), indicates that only AM2 displays bias toward cAMP at the RAMP1- and RAMP3-CLR complexes, whilst all other ligands display a preference to mobilize $i(\text{Ca}^{2+})$. Again, this is slightly different to the bias profile for HEK-293S cells. At the RAMP1-CLR complex, AM is biased toward $i(\text{Ca}^{2+})$, and AM2 is cAMP biased. For RAMP2-CLR, CGRP is biased towards $i(\text{Ca}^{2+})$ mobilization, whilst AM2 is neutral. At RAMP3-CLR all ligands are neutral, and display no bias. As before, inhibiting any signaling input from $G\alpha_i$ in HEK-293 cells, via PTX treatment, generates a relative bias profile comparable to that seen in HEK-293S cells. Thus we show that not only do RAMPs play a significant role in modulating signaling bias, but also cellular G protein content can drastically modulate any perceived bias.

Molecular modeling of CLR and GCGR in complex with RAMPs – Our experimental data suggests that the RAMPs may perform a critical role in modulating G protein coupling and bias. However we do not, as yet, have any insight to the mechanism by which this may be achieved. To at least partially address this issue we turned to the use of molecular modelling. We generate models of GCGR in complex with RAMP2 and CLR in complex with RAMP1. We used the GCGR system since it provides a reference system. The interaction between the peptide and the ligand is particularly well defined in the homologous GLP-1R system through reciprocal mutagenesis and photoaffinity labeling (28, 29) and because we have shown that the interaction between GCGR and RAMP2 affects G protein bias (25). Models taken from the last step in the 500 ns trajectory show that in both cases, the C-terminal region of the RAMP resides in the vicinity of helix 8 (H8), the intracellular ends of TM6 and TM7 and the C-terminal region of $G\alpha_s$ (Figure 10 A, B). There are differences in the orientation of the extracellular domain and the precise location of the RAMP transmembrane (TM) helix, due to the dynamic nature of the systems, the longer ‘stalk’ (the region between the ECD and TM1) in GCGR and the sequence differences between the receptors and between RAMP1 and RAMP2. There are no direct interactions between the RAMPs and the peptide ligands.

Analyses of the MD trajectories show that for GCGR and CLR, the C-terminal region of the RAMP approaches the C-terminal peptide of the G protein within the first 100 ns (Figure 10 C). For GCGR the

primary interaction is with the G protein, but there are also interactions with H8. For CLR the first part of the tail interacts with the G protein while the tip of the tail interacts with H8; in both CLR and GCGR there are also interactions with the intracellular end of TM6. The interactions are driven by a combination of steric, hydrophobic and electrostatic factors. Movies of both simulations are provided as supporting information (Movie 1 - RAMP2-GCGR- $G\alpha_s$; Movie 2 – RAMP1-CLR- $G\alpha_s$).

The extracellular end of TM7 of GCGR moves inwards under the influence of RAMP2. Analysis of distances between the extracellular end of TM2 (C α of residue K205), TM7 (C α of residue G375), the RAMP2 linker (C α of residue V145) and the peptide (C α of residue Y13) shows that the RAMP TM, TM7 and the peptide move as a collective unit towards TM2 (Figure 11), indicating a mechanism whereby the peptide ligand can influence the RAMP, and vice versa even in the absence of a direct interaction.

Discussion

The pharmacology of the CGRP family of receptors is relatively well characterized with respect to $G\alpha_s$ coupling and the resultant accumulation of cAMP (1, 12). $G\alpha_q$ and $G\alpha_i$ coupling to these receptors however, is less well characterized. Here we report the extension of the use of the *S. cerevisiae* system to investigate signaling bias in the CGRP family of receptors. These receptors are obligate heterodimers of the GPCR, namely CLR with one of three RAMPs. This dimerization adds an increased level of complexity to the system. We find that the RAMPs influence the G protein coupling in a ligand and receptor-dependent manner, in some cases radically changing ligand selectivity.

When GPA1/ $G\alpha_i$ coupling in the yeast system was compared to coupling to GPA1/ $G\alpha_s$, markedly different responses were observed for each ligand. Most significantly, at all three receptors, the rank order of potency of the ligands was altered, either being reversed or differences abolished. Efficacy calculations for each ligand in the presence of GPA1/ $G\alpha_i$ also revealed G protein directed changes in the activity of each ligand. AM2 displayed a much greater efficacy at the RAMP1-CLR heterodimer than AM, and surprisingly CGRP efficacy was greatly reduced. These data indicate that the ligands display a degree of G protein bias at each receptor and this was further supported through the construction of bias plots through calculation of $\Delta\Delta(\tau/Ka)$. The data contrasts with the established potency profiles for $G\alpha_s$ -coupled receptors observed in mammalian cells and also yeast. Whilst $G\alpha_s$ is recognized as the main signaling pathway activated by CLR-based receptors (15), the data illustrate that if $G\alpha_i$ or $G\alpha_q$ activation occurs, the conventional agonist potency ratios may lead to erroneous conclusions about the nature of the receptor. Caution should at least be taken when referring to these receptors, since it is clear that CGRP will preferentially activate the $G\alpha_s$ -coupled CGRP receptor (RAMP1-CLR), but this is not the situation when the receptor is coupled to other G proteins. Indeed, this trend is observed for all receptors in this family, with AM being the preferential ligand for both the AM₁ (RAMP2-CLR) and AM₂ (RAMP3-CLR) receptors coupled to $G\alpha_s$, but not when $G\alpha_i$ coupled. To avoid confusion we have, for the most part, described these receptors as RAMP1/2/3-CLR in this study. A further point that arises from these observations is that the reversals in potency ratios that

we observe suggest that differences in the ability of the peptides to penetrate the yeast cell wall are not a factor in contributing to our observations.

Our data also shed new light on the comparative efficacies of CGRP, AM and AM2 at the three receptors for G_{α_s} coupling. Typically they have been reported to show similar maximum responses, although there are issues with incomplete concentration-response curves (1). However, there is evidence for partial agonism of AM2 in CHO cells when RAMP2 is co-expressed with CLR (43). By its nature, measurement of efficacy is very sensitive to the cell or tissue being studied as well as the experimental protocol. In this study, the use of the yeast assay enabled us to calculate efficacy and potency values for each ligand-receptor combination for specific G protein subunits without the complication of pathway crosstalk. Our data revealed that all ligands have similar efficacies in cells expressing the RAMP1-CLR combination coupled to GPA1/ G_{α_s} . In contrast AM has a significantly increased efficacy at the RAMP2-CLR heterodimer.

The relative potencies of the three peptides at the CGRP, AM₁ and AM₂ receptors that we observe in our current studies for G_{α_s} coupling largely agree with previous observations (1 for review, 7-9, 43-44), Table 2, Figure 12). Importantly when each receptor was expressed in *S. cerevisiae* strains enabling us to measure activation of GPA1/ G_{α_s} , the rank potency order for the peptides fits the pattern observed in mammalian cells (Table 1, Figure 9), with the exception of CGRP, which displayed an unexpectedly high potency at the RAMP3-CLR heterodimer. These data indicate that, as with the GLP-1 and glucagon receptors, the yeast system is a valid model to study G protein coupling to class B GPCRs. The comparable pharmacology of the three receptors demonstrates the value of the yeast system for assessment of the effect of complex formation by GPCRs and could be applied not only to dimerization of these receptors with RAMPs but also other modifying or downstream signaling proteins.

An important consideration is whether the $G_{\alpha_i}/G_{\alpha_q}$ coupling observed in yeast has any relevance to mammalian cell systems. The yeast strains only express chimeric G proteins (containing the C-terminal 5 amino acids of the human G protein) which have been reported to be less specific when compared to equivalent G proteins expressed in mammalian cells (22). To establish the extent of G_{α_i} coupling in HEK-293 cells, we investigated cAMP production before and after PTX treatment; the greater the enhancement of cAMP production following toxin addition, the greater the extent of G_{α_i} coupling that the toxin inactivates. When compared with the coupling seen in yeast to GPA1/ G_{α_i} , whilst the correlation is not exact, there is at least a measure of agreement between the HEK-293 and yeast data, which suggests the latter, may be a guide as to what could be seen in mammalian cells, given the appropriate conditions. Comparing the relative bias plots for yeast and HEK-293 cells in Figures 7 and 9 further emphasizes this; the pattern shown for the two systems is broadly similar. As the effects of RAMPs on GPCR pharmacology are known to be sensitive to the cell line background (37, 42) and significant heterogeneity in PTX-sensitivity of CGRP has been previously reported (20, 45), it would perhaps be surprising if the HEK-293 cells were a perfect match to yeast. Indeed, as we have shown (Figure 6), in terms of the expression levels of G_{α_i} subunits, two similar HEK-293 cell lines are, in fact, very different:

HEK-239S cells appear to have a reduced level of G_{α_i} expression compared to HEK-293 cells. When combined with our observation for the PTX-sensitivity of the CLR response in HEK-293S cell lines, it becomes apparent that we need to carefully consider the G protein-content of cell lines that we utilize when we are investigating G protein-mediated signaling bias.

Our results demonstrate that the CGRP family of receptors can couple to G_{α_s} , G_{α_i} and G_{α_q} subunits. Further, using the yeast system we observed a ligand-dependent G protein coupling bias with each receptor highlighting the ability of the yeast platform to uncover potential G protein bias for other GPCRs. Importantly, this is at least partially, transferred into mammalian cells and provides an excellent starting point for subsequent investigations, into both the extent to which this bias occurs in native mammalian cells and the molecular basis for the phenomenon. Any consideration of the physiological significance of G protein promiscuity needs to consider the cellular background in which the CLR/RAMP receptor is expressed; we observe significant differences between our three cell hosts that depend, at least partly, on the G proteins they express (Figure 13). Indeed it is worth highlighting that, as a direct consequence of the reduced overall G_{α_i} content in HEK-293S cells, all 3 ligands at the CGRP family of receptors display bias towards cAMP accumulation over $i(\text{Ca}^{2+})$ release (Figure 9). Coupling to G_{α_i} (or possibly G_{α_o}) may be particularly relevant in neuronal and other electrically excitable cells where many (18-19) of the effects of PTX on CGRP have been observed (reviewed in 15). In neuronal and other cells, the direct $G_{\alpha_i}/G_{\alpha_o}$ effects on ion channels may also be particularly significant. For example, there is the potential for a complex interplay between neuronally released CGRP and the AM or AM2 peptides released locally through crosstalk between all three CLR-based receptors, with the potential of the G_{α_i} coupling to naturally limit excitation produced via G_{α_s} .

The role of $G_{\alpha_{q/11}}$ coupling in mediating responses to CGRP, AM and AM2 has not been well-investigated; the few relevant studies have examined activation of protein kinase C or release of calcium from internal stores rather than directly studying $G_{\alpha_{q/11}}$. For CGRP, a further complication is that it can also activate the amylin-1 receptor with high affinity (46) so it is not always clear that the observed effects are mediated via CLR. However, in HEK293 cells, alveolar epithelial cells, dorsal root ganglia and trigeminal ganglia, there is evidence for either release of intracellular calcium or activation of PKC alongside PKA activation (15). A similar pattern has been seen for AM in bovine aortic endothelial cells (47). Whilst evidence from PKA inhibitors such as H89 suggests that cAMP is the primary second messenger mediating many effects of CGRP (48), there is the potential for spatial and temporal modulation of this primary signal via $i(\text{Ca}^{2+})$, a possibility that remains to be explored.

By utilizing Molecular models of two diverse class B GPCR systems, namely RAMP1-CLR-CGRP and RAMP2-GCGR-glucagon systems we have gained insights into signaling bias. We believe the simulations reported here are the first molecular dynamics simulations on RAMP-GPCR heterodimers. The interaction of the RAMP TM helix with TM6/TM7 is supported by both docking experiments on CLR (27) and by studies on the secretin-GLP-1 chimeric receptor (49); this interaction remains stable throughout both 500 ns simulations of the active

receptors, with the RAMP retaining a straight helix through both simulations, despite the presence of proline(s). The interaction is primarily with TM7 and the N-terminal end of TM6. This provides some evidence that GCGR and CLR may interact with RAMP in a similar way. Despite the persistence and stability of the TM interactions, the C-terminus is quite flexible, sampling a wide region of space in both simulations. RAMP2 interacts primarily with the C-terminus of $G\alpha_s$ while RAMP1 interacted primarily with H8 but also made contacts with TM6 and most importantly $G\alpha_s$. These simulations therefore indicate that the RAMP could affect the bias shown in G protein coupling by CLR either by direct interaction, and, or, allosterically by altering the orientation of TM6 and TM7 or H8. These simulations were carried out on a model of the active receptor in complex with a C-terminal fragment of $G\alpha_s$ (R374 to L394). The C-terminal helix of $G\alpha_s$ sits above the face of the G protein. Models of RAMP2-GCGR in complex with the G protein heterotrimer indicate that the RAMP could also interact directly with residues around G353 of $G\alpha_s$ (results not shown).

In addition, allosteric effects of the RAMP linker may alter the extracellular face of the receptor (as seen in CLR with RAMP2 and RAMP3 (27)) and these effects could be transmitted to the intracellular end of the helix. In our simulations we see some evidence for the top of TM7 moving in toward the TM bundle under pressure of the RAMP (Figure 11) as part of a collective unit comprised of TM7, the peptide and the RAMP TM. This concerted movement provides a possible mechanism whereby the influence of the ligand can be conveyed to the RAMP and thereby affect the bias via interactions of the C-terminus of the RAMP. The inward movement of the extracellular end of TM7 has been explicitly linked to activation (50), but movement of TM6 and / or H8 under the influence of the RAMP may also affect bias and activation. Thus we suggest that RAMPs have the potential to interact allosterically with not only the GPCR but also the bound G protein. This leads to the possibility that, upon ligand binding the RAMPs contribute to the G protein bias. In order to confirm this we aim to extend this project to investigate all ligand-RAMP-CLR-G protein complexes, to further elucidate the roles RAMPs play in modulating G protein coupling and bias at the CGRP family of receptors.

Finally, we suggest that this study has broader implications. Our results shown here are similar to those described for the GCGR (25) in that RAMPs alter the ability of peptides to stimulate different G proteins. However, as we have shown significant pharmacological differences can be observed in differing recombinant cell lines, and expression systems. These differences can be explained through several factors; firstly these systems rely upon over expression of the receptor and chaperone proteins under study, and secondly upon cellular content of further downstream signaling proteins, such as G proteins. It is therefore important that findings in systems such as those explained here are further validated. This would be best achieved in cell lines endogenously expressing the GPCR, and RAMP, of interest. This is thus something we aim to undertake as a follow up to the work presented here, for CLR/RAMP complexes. It is clear that there is a complex interplay between the ligand, the RAMP and the CLR that alters G protein activation for these receptors. Further, our data adds to the growing wealth of literature suggesting that many ligands for

class B GPCRs display either $G\alpha_s$ or $G\alpha_i$ signaling preference. To date this ligand-engendered bias has been observed for receptors binding corticotropin-releasing factor, urocortin 1, GLP-1 and glucagon (24-25, 51). In this study, the yeast growth assay system was able to provide a valuable indication of the potential of the CGRP family of receptors to couple to either $G\alpha_s$ or $G\alpha_i$ when stimulated by CGRP, AM or AM2, allowing us to uncover novel G protein signaling preferences for each ligand. We can therefore conclude that this system is a good platform with which to explore the effect of RAMP dimerization to other members of the class B GPCRs.

Methods

Materials - Human (h) α CGRP, hAM and hAM2 (1-47) were purchased from Bachem (Bubendorf, Switzerland) and made to 1 mM stocks in water containing 1% BSA. Yeast nitrogen base and yeast extract were purchased from Difco (Franklin Lakes, NJ). Fluorescein-Di- β -D-glucopyranoside (FDGlu) was purchased from Invitrogen (Paisley, UK). Forskolin was from Tocris Bioscience (Wiltshire, UK), YM-254890 was supplied by alpha laboratories (Hampshire, UK). Both ALPHAScreen and LANCE® cAMP detection assay kit and all reagents were from PerkinElmer (Boston, MA, USA).

Expression Constructs - To enable expression of the human CLR we used either a previously described (25) myc-tagged cDNA construct provided by Dr Michel Bouvier (University of Montreal, Canada) or a human CLR with an N-terminal haemagglutinin (HA) epitope tag. All human FLAG-tagged RAMPs were used as described previously (37).

Yeast strain construction and assay - General yeast procedures were performed as described previously (22, 24). The human CLR was introduced into yeast cells under the control of the *PGK* promoter using a plasmid containing *ura3* (pDT-PGK). The three human RAMPs were introduced into yeast under the control of the *GAPDH* promoter using plasmids containing *leu2* (p425-GPD) (25). *S. cerevisiae* dual reporter strains expressing chimeras of the yeast GPA1, 1-467, (GPA1/ $G\alpha$) with the five C-terminal amino acids of 11 human G proteins representing $G\alpha_s$, $G\alpha_{16}$, $G\alpha_q$, $G\alpha_o$, $G\alpha_{i1/2}$, $G\alpha_{i3}$, $G\alpha_z$, $G\alpha_{12}$, $G\alpha_{13}$, and $G\alpha_{14}$ (MMY84-MMY93) were used in this study (52). The human CLR and RAMPs were transformed into yeast cells (at a ratio of 1:1 to enable equal expression) using the lithium acetate/single-stranded DNA/polyethylene glycol method as previously described (53). Positive transformants were selected and maintained on synthetic dropout (SD) media lacking both uracil and leucine (SD-URA-LEU). Receptor signaling was measured using the yeast growth assay as described previously (24). Cell growth was initially performed in SD-URA-LEU media at 30°C to select cells only expressing both plasmids. Cells were then cultured to remove basal activity in SD-URA-LEU-HIS media overnight at 30°C and assayed using media supplemented with FDGlu. Fluorescein signal was detected as an increase in fluorescence (excitation wavelength = 485 nm, emission wavelength = 535 nm) as a measure of growth. Different concentrations of ligand (0.01 nM - 100 μ M) were assayed using 96-well plates and fluorescence detected using a TECAN Infinite M200 microplate reader (TECAN Ultra Evolution, Reading, UK) or a Mithras LB940 microplate reader (Berthold Technologies, Harpenden, UK) for 20 h. Positive isolates were selected upon their ability to grow in

SD-URA-LEU-HIS media, above basal, when stimulated with 10 μ M CGRP or AM as appropriate for the RAMP-CLR complex being studied. Chimeric strains were deemed not to functionally couple when $n > 16$ isolates had been assayed and none showed growth above basal levels. In this study functional couplings were only observed for MMY84, MMY86 and MMY88 representing G_{α_s} , $G_{\alpha_{i1/2}}$ and G_{α_q} respectively.

Mammalian Cell Culture and Transfection - HEK-293 cells, provided by Dr Jürgen Müller (University of Aston), were cultured in Dulbecco's Modified Eagle Medium (DMEM) supplemented with 10% heat inactivated fetal bovine serum (FBS) and kept in a 37°C, humidified 95% air, 5% CO₂ incubator. HEK-293S cells (a gift from AstraZeneca) were cultured in DMEM supplemented with 8% heat inactivated FBS and kept in a 37°C humidified 95% air, 5% CO₂ incubator. HEK-293 cells were transfected with Fugene 6 (Roche) in accordance with the manufacturer's instructions using a 1:3 (w:v) DNA:Fugene ratio and a 1:1 ratio of RAMP to CLR. HEK-293S cells were seeded into 96 well poly-D-lysine coated plates at a density of 15,000 cells per well (determined using a Countess Counter™, Invitrogen) one day prior to transfection. HEK-293S cells were transiently transfected as described previously (38) using a 1:1 ratio of RAMP to CLR. Transfected cell lines were grown for 24-48 h prior to assaying. Where appropriate, PTX (200 ng/ml) was added to ADP-ribosylate G_{α_i} for 16 h prior to assaying, thereby uncoupling receptor-mediated G_{α_i} -dependent inhibition of cAMP production.

cAMP accumulation assays - Transfected HEK-293 cells were washed in PBS, resuspended in stimulation buffer (PBS containing 0.1% BSA and 0.5 mM IBMX) and seeded at 2000 cells per well in 384-well white Optiplates. Ligands were added in the range of 1 pM to 1 mM and cAMP accumulation was measured after 30 min stimulation using LANCE® cAMP Detection Kit (PerkinElmer, MA, USA). We have previously found 30 min stimulation to be the optimum time for assaying cAMP accumulation for family B GPCRs (24, 25). Plates were read using a Mithras LB 940 multimode microplate reader (Berthold technologies, Germany). HEK-293S cells were assayed for cAMP accumulation as described (54). Values were converted to concentration using a cAMP standard curve performed in parallel.

Calcium mobilization assays - Transfected HEK-293 cells were grown to confluence in black, clear bottomed, 96 well plates. On the day of assay cells were washed with calcium free HBSS and incubated for 1 h, at room temperature, in the presence of 10 μ M Fluo-4/AM (Invitrogen, Paisely, UK) containing 2.5 mM probenecid. Cells were then washed, followed by addition of 100 μ l Ca²⁺ free HBSS. Ligands were robotically added using a Mithras LB 940 multimode microplate reader, in the range of 10 pM to 1 μ M, and fluorescence determined immediately post-injection, with an excitation wavelength set to 485 nm and an emission wavelength set to 535 nm. Recordings were obtained every 0.5 s for 120 s. Peak magnitude was calculated using five-point smoothing, followed by correction against background fluorescence. The peak was used to generate concentration-response curves and normalized relative to 10 μ M ionomycin. In order to determine the roles played by $G_{\alpha_{q11}}$ in i(Ca²⁺) mobilization, cells were pretreated (for 30 mins) with 100 nM YM-254890 to inhibit $G_{\alpha_{q11}}$ signaling (42).

Reverse-transcriptase-polymerase chain reaction (RT-PCR) - RNA was extracted from HEK-293 and HEK-293S cells using RNeasy 4 Polymerase chain reaction (PCR) kit (ThermoFisher, Paisely, UK) as per the manufacturers protocol. All RNA samples were treated with DNaseI to remove contaminating genomic DNA. Reverse transcription was performed using a QuantiTect reverse transcription kit (Qiagen, Manchester, UK). The PCR amplification was performed as described previously (55) using gene-specific primers to human G_{α} subunits;

G_{α_s} ;	forward	-
CGACGACACTCCCGTCAAC,	reverse	-
CCCGGAGAGGGTACTTTTCCT (PrimerBank ID - 3297877a1, (55)),	$G_{\alpha_{i1}}$;	forward
TTAGGGCTATGGGGAGGTTGA,	reverse	-
GGTACTCTCGGGATCTGTTGAAA (PrimerBank ID 156071490c1, (55)),	$G_{\alpha_{i2}}$;	forward
TACCGGGCGGTTGTCTACA,	reverse	-
GGGTCGGCAAAGTCGATCTG (PrimerBank ID - 261878574c1, (55)),	$G_{\alpha_{i3}}$;	forward
ATCGACCGCAACTTACGGG,	reverse	-
AGTCAATCTTTAGCCGTCCTCA (PrimerBank ID - 169646784c1, (55)),	G_{α_q} ;	forward
TGGGTCAGGATACTCTGATGAAG,	reverse	-
TGTGCATGAGCCTTATTGTGC (PrimerBank ID - 312176363c1, (55)),	$G_{\alpha_{11}}$;	forward
GGCTTCACCAAGCTCGTCTAC,	reverse	-
CACTGACGTACTGATGCTCG (PrimerBank ID - 115511048c1, (55)),	G_{α_z} ;	forward
GGTCCCGGAGAATTGACCG,	reverse	-
ATGAGGGGCTTGTACTIONCTTG (PrimerBank ID - 45580725c1, (55)),	G_{α_0} ;	forward
GGAGCAAGGCGATTGAGAAAA,	reverse	-
GGCTTGTACTIONTTTACGTCT (PrimerBank ID - 162461737c1, (55)),	$G_{\alpha_{12}}$;	forward
CCGCGAGTTCGACCAGAAG,	reverse	-
TGATGCCAGAATCCCTCCAGA (PrimerBank ID - 42476110c1, (55)),	$G_{\alpha_{13}}$;	forward
CAGCAACGCAAGTCCAAGGA,	reverse	-
CCAGCACCCCTACACTTTGA (PrimerBank ID - 215820623c1, (55)),	$G_{\alpha_{14}}$;	forward
GAGCGATGGACACGCTAAGG,	reverse	-
TCCTGTCGTAACACTCCTGGA (PrimerBank ID - 222418795c1, (55)),	$G_{\alpha_{15}}$;	forward
CCAGGACCCCTATAAAGTGACC,	reverse	-
GCTGAATCGAGCAGGTGGAAT (PrimerBank ID 156104882c1, (55)),	glyceraldehyde 3-phosphate dehydrogenase (GAPDH);	forward
AATGGGCAGCCGTTAGGAAA,	reverse	-
GCGCCCAATACGACCAAATC.		

All products were resolved on a 2% agarose gel and imaged using a G:Box iChemi gel documentation system utilizing Gene Tool analysis software (Syngene, Cambridge, UK), densitometry was performed using Gene Tool.

Molecular Modelling - Models of the GCGR in complex with RAMP2 and CLR in complex with RAMP1 were based on the previously reported models of GLP-1R in complex with GLP-1 and CLR in complex with RAMP2/3 respectively (27-29); these models were built using modeler 9.16 (57) from the GCGR and CRFR X-ray structures of the TM domain (58, 59), the X-ray structures of the extracellular domain (ECD) (60, 61) and NMR structures of closely related peptides (62, 63). The helical region of the CGRP peptide was structurally aligned to the corresponding region in GLP-1 based on the sequence alignment (27) because the position of the GLP1 helix within GLP-1R is well defined by experimentation; the initial models are available as supporting information. The RAMP-GPCR complexes were placed in a hydrated POPC membrane using the

CHARMM GUI (64) to generate a system containing 20,482 and 28,013 TIP3P water molecules (65), as well as 183 and 243 lipid molecules for the RAMP2-GCGR and RAMP1-CLR heterodimers, respectively. The histidine protonation was determined using the PDB2PQR server (66). The AMBERS99 force field parameters for the protein (67), and the lipid14 force field parameters for POPC (68, 69) were added using ambertools (70). Molecular dynamics simulations were run for 500 ns at 298 K using ACEMD (71).

Data Analysis - Data analysis for cAMP assays was performed in GraphPad Prism 6.0f (San Diego, CA, USA). Data were fitted to obtain concentration–response curves using either the three-parameter logistic equation (for pEC₅₀ values), or the operational model for partial agonism (34) to obtain values of efficacy (log τ) and the equilibrium dissociation constant (log k_A). These values were then used to quantify signaling bias as change in log (τ/k_A) relative to the natural cognate ligand for the respective receptor (41). We denoted these as CGRP for CLR with RAMP1, and AM for CLR with either RAMP2 or RAMP3. Statistical differences were analyzed using one-way ANOVA or Student's t-test as appropriate with post-hoc Bonferroni's or Dunnett's multiple comparisons, a probability of (p) < 0.05 was considered significant. Correlations between pEC₅₀ values, for cAMP assays, of HEK-293 and HEK-293S cells were assessed by scatter plot and Pearson's correlation coefficient (r). For the RT-PCR, normalization to the internal standard GAPDH was performed to reduce variance and enable comparison between different cell lines. In order to quantitate the ligand-dependent response in the yeast system, a strain lacking GPA1 (MMY11), grown in rich media, was used as a standard (72). As GPA1 is not present in this strain, the G $\beta\gamma$ subunits are unregulated and free to signal, allowing us to determine the maximal response of our system. E_{max} values are reported as a percentage of this maximum response and statistical analysis has been performed on this data. For the mammalian cell based assays, data analysis was carried out as for the yeast curves. To account for the day-to-day variation experienced from transient transfections we have used the maximal level of cAMP accumulation from cells in response to 100 μ M forskolin stimulation as our reference, and 10 μ M

ionomycin for i(Ca²⁺) assays. E_{max} values from these curves are reported as a percentage of these controls and all statistical analysis has been performed on this data. Where appropriate the operational model for partial agonism (34) was used to obtain values of efficacy (log τ) and equilibrium dissociation constant (log K_A). In both cases, this normalization removes the variation due to differences in transfection or transformation but retains the variance for control values. The means of individual experiments were combined to generate the curves shown.

Acknowledgements

This work was supported by the National Heart Foundation of New Zealand (H.W.), the School of Biological Sciences, University of Auckland seed fund (H.W.), the BBSRC (G.L. - BB/M00015X/1), (D.P. - BB/M000176/1), (C.A.R. - BB/M006883/1), a BBSRC Doctoral Training Partnership (M.H. - BB/JO14540/1), an MRC Doctoral Training Partnership (I.W. - MR/J003964/1), a Warwick Impact Fund (C.W., G.L.), a Warwick Research Development Fund (C.W., G.L.) grant number (RD13301) and the Warwick Undergraduate Research Scholarship Scheme (A.S and R.H).

Conflict of Interest

The authors declare they have no conflicts of interest with the contents of this article.

Author Contributions

CW, HAW and GL conceived and designed the research; CW, AS, RH performed the yeast experiments, IW and HAW performed the mammalian assays; MH performed the RT-PCR; CAR, JCM, DAW carried out the computational chemistry, SJD provided yeast strains; CW, DRP, HAW, JCM and CAR and GL analyzed data; CW, DRP, HAW, JCM, CAR and GL wrote manuscript; SJD revised and edited the manuscript.

References

1. Hong Y, Hay DL, Quirion R, Poyner DR (2012). The pharmacology of Adrenomedullin 2/Intermedin. *Br J Pharmacol* **166**: 110-120.
2. Russell FA, King R, Smillie SJ, Kodji X, Brian SD (2014). Calcitonin gene-related peptide: physiology and pathophysiology. *Physiol Rev* **94**:1099-1142
3. Edvinsson L, Warfvinge K (2013). CGRP receptor antagonism and migraine therapy. *Curr Protein Pept Sci* **14**: 386-392.
4. Kato J, Kitamura K (2015). Bench-to-bedside pharmacology of adrenomedullin. *Eur J Pharmacol* **764**: 140-148.
5. Fritz-Six KL, Dunworth WP, Li M, Caron KM (2008). Adrenomedullin signaling is necessary for murine lymphatic vascular development. *J Clin Invest* **118**: 40-50.
6. Ichikawa-Shindo Y, Sakurai T, Kamiyoshi A, Kawate H, Iinuma N, Yoshizawa T, *et al.* (2008). The GPCR modulator protein RAMP2 is essential for angiogenesis and vascular integrity. *J Clin Invest* **118**: 29-39.
7. Roh J, Chang CL, Bhalla A, Klein C, Hsu SY (2004). Intermedin is a calcitonin/calcitonin gene-related peptide family peptide acting through the calcitonin receptor-like receptor/receptor activity-modifying protein receptor complexes. *J Biol Chem* **279**: 7264-7274.
8. Holmes D, Campbell M, Harbinson M and Bell D (2013). Protective effects of intermedin on cardiovascular, pulmonary and renal diseases: comparison with adrenomedullin and CGRP. *Curr Protein Pept Sci* **14**: 294-329
9. Takei Y, Inoue K, Ogoshi M, Kawahara T, Bannai H, Miyano S (2004). Identification of novel adrenomedullin in mammals: a potent cardiovascular and renal regulator. *FEBS Lett* **556**: 53-58.
10. Smillie SJ, Brian SD (2011). Calcitonin gene-related peptide (CGRP) and its role in hypertension. *Neuropeptides* **45**: 93-104
11. Kataoka Y, Miyazaki S, Yasuda S, Nagaya N, Noguchi T, Yamada N, *et al.* (2010). The first clinical pilot study of intravenous adrenomedullin administration in patients with acute myocardial infarction. *J Cardiovasc Pharmacol* **56**: 413-419.
12. Poyner DR, Sexton PM, Marshall I, Smith DM, Quirion R, Born W, *et al.* (2002). International Union of Pharmacology. XXXII. The mammalian calcitonin gene-related peptides, adrenomedullin, amylin, and calcitonin receptors. *Pharmacol Rev* **54**: 233-246.
13. LM, Fraser NJ, Main MJ, Wise A, Brown J, Thompson N, *et al.* (1998). RAMPs regulate the transport and ligand specificity of the calcitonin-receptor-like receptor. *Nature* **393**: 333-339.
14. Hay DL, Poyner DR, Smith DM (2003). Desensitisation of adrenomedullin and CGRP receptors. *Regul Pept* **112**: 139-145.
15. Walker CS, Conner AC, Poyner DR, Hay DL (2010). Regulation of signal transduction by calcitonin gene-related peptide receptors. *Trends Pharmacol Sci* **31**: 476-483.
16. Woolley MJ, Conner AC (2013). Comparing the molecular pharmacology of CGRP and adrenomedullin. *Curr Protein Pept Sci* **14**: 358-374.
17. Wiley JW, Gross RA, MacDonald RL (1992). The peptide CGRP increases a high-threshold Ca^{2+} current in rat nodose neurones via a pertussis toxin-sensitive pathway. *J Physiol* **455**: 367-381.
18. Disa J, Parameswaran N, Nambi P, Aiyar N (2000). Involvement of cAMP-dependent protein kinase and pertussis toxin-sensitive G-proteins in CGRP mediated JNK activation in human neuroblastoma cell line. *Neuropeptides* **34**: 229-233.
19. Kim D (1991). Calcitonin-gene-related peptide activates the muscarinic-gated K^{+} current in atrial cells. *Pflugers Arch* **418**: 338-345.
20. Main MJ, Brown J, Brown S, Fraser NJ, Foord SM (1998). The CGRP receptor can couple via pertussis toxin sensitive and insensitive G proteins. *FEBS Lett* **441**: 6-10.
21. Kuwasako K, Kitamura K, Nagata S, Hikosaka T, Kato J (2010). Function of the cytoplasmic tail of human calcitonin receptor-like receptor in complex with receptor activity-modifying protein 2. *Biochem Biophys Res Commun* **392**: 380-385.

22. Dowell SJ, Brown AJ (2002). Yeast assays for G-protein-coupled receptors. *Receptors Channels* **8**: 343-352.
23. Ladds G, Goddard A, Davey J (2005). Functional analysis of heterologous GPCR signalling pathways in yeast. *Trends Biotechnol* **23**: 367-373.
24. Weston C, Poyner D, Patel V, Dowell S, Ladds G (2014). Investigating G protein signalling bias at the glucagon-like peptide-1 receptor in yeast. *Br J Pharmacol* **171**: 3651-3665.
25. Weston C, Lu J, Li N, Barkan K, Richards GO, *et al.* (2015). Modulation of glucagon receptor pharmacology by RAMP2. *J Biol Chem* **290**: 23009-23022.
26. Miret JJ, Rakhilina L, Silverman L, Oehlen B (2002). Functional expression of heteromeric calcitonin gene-related peptide and adrenomedullin receptors in yeast. *J Biol Chem* **277**: 6881-6887.
27. Watkins HA, Chakravarthy M, Abhayawardana RS, Gingell JJ, Garelja M, *et al.* (2016). Receptor Activity-Modifying Proteins 2 and 3 generate adrenomedullin receptor subtypes with distinct molecular properties. *J Biol Chem* **291**: 11657-11675.
28. Wootten D, Reynolds CA, Smith KJ, Mobarec JC, Koole C *et al.* (2016). The extracellular surface of the GLP-1 receptor is a molecular trigger for biased agonism. *Cell* **165**: 1632-43.
29. Wootten D, Reynolds, CA, Koole C, Smith KJ, Mobarec JC, *et al.* (2016) A hydrogen-bonded polar network in the core of the glucagon-like peptide-1 receptor is a fulcrum for biased agonism: lessons from Class B crystal structures. *Mol Pharmacol* **89**: 335-47.
30. Yang D, de Graaf, C, Yang L, Song G, Dai A, *et al.* (2016) Structural determinants of binding the seven-transmembrane domain of the glucagon-like peptide-1 receptor (GLP-1R). *J Biol Chem* **291**: 12991-3004.
31. Yang L, Yang D, de Graaf C, Moeller A, West GM, *et al.* (2015) Conformational states of the full-length glucagon receptor. *Nat comm* **6**: 7859.
32. Singh R, Ahalawat N, Murarka RK (2015) Activation of corticotropin-releasing factor 1 receptor: insights from molecular dynamics simulations. *J Phys Chem B* **119**: 2806-17.
33. Li Y, Sun J, Li D, Lin J. (2016) Activation and conformational dynamics of a class B G-protein-coupled glucagon receptor. *Phys Chem Chem Phys* **18**: 12642-50.
34. Black JW, Leff P (1983). Operational models of pharmacological agonism. *Proc R Soc Lond B Biol Sci* **220**: 141-162.
35. Lin YC, Boone M, Meuris L, Lemmens I, Van Roy N, Soete A, *et al.* (2014). Genome dynamics of the human embryonic kidney 293 lineage in response to cell biology manipulations. *Nat Commun* **5**: 4767.
36. Stillman BW, Gluzman Y (1985). Replication and supercoiling of simian virus 40 DNA in cell extracts from human cells. *Mol Cell Biol* **5**: 2051-2060.
37. Wootten DL, Lindmark H, Kadmiel M, Willcockson HH, Caron KM, Barwell J, Drmota T, Poyner D (2013). Receptor activity modifying proteins (RAMPs) interact with the VPAC 2 receptor and CRF1 receptors and modulate their function. *Br J Pharmacol* **168**: 822-834.
38. Qi T, Dong M, Watkins HA, Wootten D, Miller LJ, Hay DL (2013). Receptor activity-modifying protein-dependent impairment of calcitonin receptor splice variant $\Delta(1-47)$ hCT((a)) function. *Br J Pharmacol* **168**: 644-657.
39. Hay DL, Walker, CS, Gingell JJ, Ladds G, Reynolds CA, Poyner DR (2016). Receptor Activity Modifying Proteins; multifunctional G protein-coupled receptor accessory proteins. *Biochem Soc Trans* **44**: 568-573.
40. Atwood BK, Lopez J, Wagner-Miller, J Mackie K, Straiker A (2011). Expression of G protein-coupled receptors and related proteins in HEK293, AtT20, BV2, and N18 cell lines as revealed by microarray analysis. *BMC genomics* **12**: 14
41. Figueroa KW, Griffin MT, Ehlert FJ (2009). Selectivity of agonists for the active state of M1 to M4 muscarinic receptor subtypes. *J Pharmacol Exp Ther* **328**: 331-342.
42. Takasaki J, Saito T, Taniguchi M, Kawasaki T, Moritani Y, Hayashi K, Kobori M (2004) A novel *Gaq/11*-selective inhibitor. *J Biol Chem* **279**: 47438-47445.

43. Wunder F, Rebmann A, Geerts A, Kalthof B (2008). Pharmacological and kinetic characterization of adrenomedullin 1 and calcitonin gene-related peptide 1 receptor reporter cell lines. *Mol Pharmacol* **73**: 1235-1243.
44. Watkins HA, Walker CS, Ly KN, Bailey RJ, Barwell J, Poyner DR, *et al.* (2014). Receptor activity-modifying protein-dependent effects of mutations in the calcitonin receptor-like receptor: implications for adrenomedullin and calcitonin gene-related peptide pharmacology. *Br J Pharmacol* **171**: 772-788.
45. Aiyar N, Disa J, Stadel JM, Lysko PG (1999). Calcitonin gene-related peptide receptor independently stimulates 3',5'-cyclic adenosine monophosphate and Ca²⁺ signaling pathways. *Mol Cell Biochem* **197**: 179-185.
46. Christopoulos G, Perry KJ, Morfis M, Tilakaratne N, Gao Y, Fraser NJ, Main MJ, Foord SM, Sexton PM (1999) Multiple amylin receptors arise from receptor activity-modifying protein interaction with the calcitonin receptor gene product. *Mol Pharmacol* **56**: 235-242
47. Shimekake Y, Nagata K, Ohta S, Kambayashi Y, Teraoka H, Kitamura K, Eto T, Kangawa K, Matsuo H. (1995) Adrenomedullin stimulates two signal transduction pathways, cAMP accumulation and i(Ca²⁺) mobilization, in bovine aortic endothelial cells. *J Biol Chem* **270**: 4412-4417.
48. Permpoonputtana K, Porter JE, Govitrapong (2016). Calcitonin gene-related peptide mediates an inflammatory response in Schwann cells via cAMP-dependent ERK signaling cascade. *Life Sci* **144**: 19-25
49. Harikumar KG, Simms J, Christopoulos G, Sexton PM, Miller LJ (2009) Molecular Basis of Association of Receptor Activity-Modifying Protein 3 with the Family B G Protein-Coupled Secretin Receptor. *Biochemistry* **48**: 11773-11785.
50. Rasmussen SGF, DeVree BT, Zou YZ, Kruse AC, Chung KY, *et al* (2011) Crystal structure of the beta(2) adrenergic receptor-Gs protein complex. *Nature* **477**: 549-U311.
51. Ladds G, Davis K, Hillhouse EW, Davey J (2003). Modified yeast cells to investigate the coupling of G protein-coupled receptors to specific G proteins. *Mol Microbiol* **47**: 781-792.
52. Brown AJ, Goldsworthy SM, Barnes AA, Eilert MM, Tcheang L, Daniels D, *et al.* (2003). The Orphan G protein-coupled receptors GPR41 and GPR43 are activated by propionate and other short chain carboxylic acids. *J Biol Chem* **278**: 11312-11319.
53. Gietz RD, Schiestl RH (2007). Quick and easy yeast transformation using the LiAc/SS carrier DNA/PEG method. *Nat Protoc* **2**: 35-37.
54. Gingell JJ, Qi T, Bailey RJ, Hay DL (2010). A key role for tryptophan 84 in receptor activity-modifying protein 1 in the amylin 1 receptor. *Peptides* **31**: 1400-1404.
55. Ladds G, Zervou S, Vatish M, Thornton S, Davey J (2009). Regulators of G protein signalling proteins in the human myometrium. *Eur J Pharmacol* **610**: 23-28
56. Spandidos A, Wang X, Wang H and Seed B (2010). PrimerBank: a resource of human and mouse PCR primer pairs for gene expression detection and quantification. *Nucl Acids Res* **38**: D729-799
57. Eswar N, Webb B, Marti-Renom MS, Madhusudham DE, Shen MY, *et al* (2007). Comparative Protein Structure Modeling with MODELLER. *Curr Protoc Bioinformatics* **2.9.1-2.9.31**.
58. Siu FY, He M, de Graaf C, Han GW, Yang D, Zhang Z, Zhou C, *et al* (2013). Structure of the human glucagon class B G-protein-coupled receptor. *Nature* **499**: 444-449.
59. Hollenstein K, Kean J, Bortolato A, Cheng RKY, Dore AS, *et al* (2013). Structure of class B GPCR corticotropin-releasing factor receptor 1. *Nature* **499**: 438-443.
60. Booe JM, Walker CS, Barwell J, Kuteyi G, Simms J, *et al* (2015). Structural Basis for Receptor Activity-Modifying Protein-Dependent Selective Peptide Recognition by a G Protein-Coupled Receptor. *Mol cell* **58**:1040-1052.
61. Koth CM, Murray JM, Mukund S, Madjidi A, Minn A, *et al* (2012). Molecular basis for negative regulation of the glucagon receptor. *Proc Natl Acad Sci U S A* **109**: 14393-14398.
62. Hoang HN, Song K, Hill TA, Derksen DR, Edmonds DJ, *et al* (2015). Short Hydrophobic Peptides with Cyclic Constraints Are Potent Glucagon-like Peptide-1 Receptor (GLP-1R) Agonists. *J Med Chem* **58**: 4080-4085.

63. Perez-Castells J, Martin-Santamaria S, Nieto L, Ramos A, Martinez A, *et al* (2012). Structure of micelle-bound adrenomedullin: a first step toward the analysis of its interactions with receptors and small molecules. *Biopolymers* **97**: 45-53.
64. Jo S, Kim T, Iyer VG, Im W (2008). CHARMM-GUI: a web-based graphical user interface for CHARMM. *J Comput Chem* **29**: 1859-1865.
65. Jorgensen WL, Chandrasekhar J, Madura JD, Impey RW, Klein ML (1983). Comparison of Simple Potential Functions for Simulating Liquid Water. *J Chem Phys.* **79**: 926-935
66. Dolinsky TJ, Nielsen JE, McCammon JA, Baker NA (2004). PDB2PQR: an automated pipeline for the setup of Poisson-Boltzmann electrostatics calculations. *Nucleic Acids Res* **32**: W665-W667.
67. Hornak V, Abel R, Okur A, Strockbine B, Roitberg A, Simmerling C (2006). Comparison of multiple Amber force fields and development of improved protein backbone parameters. *Proteins* **65**: 712-725.
68. Walker RC, Dickson CJ, Madej BD, Skjevik AA, Betz RM, Teigen K, Gould IR (2014). Amber lipid force field: Lipid14 and beyond. *Abstr Pap Am Chem S* 248.
69. Dickson CJ, Madej BD, Skjevik AA, Betz RM, Teigen K, Gould IR, Walker RC (2014). Lipid14: The Amber Lipid Force Field. *J Chem Theory Comput* **10**: 865-879.
70. Case DA, Betz RM, Botello-Smith W, Cerutti DS, Cheatham TE, III, *et al* (2016), AMBER 2016, University of California, San Francisco.
71. Harvey MJ, Giupponi G, De Fabritiis G (2009) ACEMD: Accelerating Biomolecular Dynamics in the Microsecond Time Scale. *J Chem Theory Comput* **5**: 1632-1639.
72. Brown AJ, Dyos SL, Whiteway MS, White JH, Watson MA, Marzioch M, *et al.* (2000). Functional coupling of mammalian receptors to the yeast mating pathway using novel yeast/mammalian G protein alpha-subunit chimeras. *Yeast* **16**: 11-22.

Figure legends

Figure 1. Functional expression of CLR co-transformed with all three RAMPs in yeast cells. Dose response curves to CGRP, AM and AM2 were constructed in yeast strains containing the GPA1/ $G\alpha_s$ chimera and expressing CLR with (A), RAMP1 ($n = 6$) (B), RAMP2 ($n = 7$) and (C), RAMP3 ($n = 8$). Reporter gene activity was determined following 20 h stimulation with each ligand. Data are expressed as percentage of the maximum response observed in a yeast strain MMY11 (lacking GPA1) and are means \pm SEM of n individual data sets. (D) Bar chart showing the efficacy of each ligand for each RAMP-CLR combination as determined via application of the operational model of receptor agonism ((34); Table 1). Data were determined as statistically different from the cognate ligand for each receptor (*, $p < 0.05$, **, $p < 0.01$, ***, $p < 0.001$) using a one-way ANOVA with Bonferroni's post-test.

Figure 2. Expression of CLR in combination with each RAMP generates functional $G\alpha_s$ -coupled receptors in HEK-293 cells. cAMP accumulation was determined in HEK-293 cells transiently transfected with the CLR and (A), RAMP1 ($n = 11$) (B), RAMP2 ($n = 8$) and (C), RAMP3 ($n = 9$) following 30 min stimulation with CGRP, AM and AM2. Data are expressed as percentage maximal cAMP production, determined using 100 μ M forskolin stimulation and are means \pm SEM of n individual data sets. (D) Bar chart showing the efficacy of each ligand for each RAMP-CLR combination as determined via application of the operational model of receptor agonism (34). Data were determined as statistically different from the cognate ligand for each receptor (*, $p < 0.05$, **, $p < 0.01$) using a one-way ANOVA with Bonferroni's post-test.

Figure 3. Co-transformation of CLR with all three RAMPs in yeast cells generates receptors that functionally couple to the $G\alpha_i$ chimera. Dose response curves to CGRP, AM and AM2 were constructed in yeast strains containing the GPA1/ $G\alpha_i$ chimera and expressing CLR with (A), RAMP1 ($n = 6$) (B), RAMP2 ($n = 6$) and (C), RAMP3 ($n = 7$). Reporter gene activity was determined following 20 h stimulation. All data are expressed as percentage of the maximum response observed in a yeast strain MMY11 (lacking GPA1) and are means \pm SEM of n individual data sets. (D) Bar chart showing the efficacy of each ligand for each RAMP-CLR combination as determined via application of the operational model of receptor agonism ((34); Table 1). Data were determined as statistically different from the cognate ligand for each receptor (*, $p < 0.05$, **, $p < 0.01$, ***, $p < 0.001$, ****, $p < 0.0001$) using a one-way ANOVA with Bonferroni's post-test.

Figure 4. CLR in combination with each RAMP generates receptors that display PTX-sensitive effects in response to ligand stimulation. cAMP accumulation was determined in the presence (treated) and absence (untreated) of PTX, from HEK-293 cells transiently transfected with CLR and (A), RAMP1 ($n = 6$) (B), RAMP2 ($n = 5$) and (C), RAMP3 ($n = 5$). Cells were stimulated for 30 min with CGRP, AM and AM2; data are expressed as percentage of the maximal cAMP production as determined using 100 μ M forskolin stimulation in presence of PTX and are means \pm SEM of n individual data sets.

Figure 5. RAMP-CLR responses appear PTX-insensitive when assayed using HEK-293S cells. cAMP accumulation was determined in the presence (treated) and absence (untreated) of PTX, from HEK-293S cells transiently transfected with CLR and (A), RAMP1 ($n = 5$) (B), RAMP2 ($n = 5$) and (C), RAMP3 ($n = 5$). Cells were stimulated for 30 min with CGRP, AM and AM2; data are expressed as percentage of the maximal cAMP production as determined using 100 μ M forskolin stimulation in presence of PTX and are means \pm SEM of n individual data sets.

Figure 6. Reduced $G\alpha_i$ expression in HEK-293S cell lines leads to PTX-sensitive. (A) Expression profiles of $G\alpha$ genes were assessed in HEK-293 and HEK-293S cells. RNA was extracted from cells and treated with DNase1 to remove genomic DNA contamination. $G\alpha$ gene expression was examined by RT-PCR using gene-specific primers. The * indicates a lack of detectable transcript for $G\alpha_{i2}$. The band shown is a non-specific product as confirmed by DNA sequencing. (B) Semi-quantitative expression (relative to GAPDH) for the $G\alpha$ genes from (A) ($n = 4$). Statistical difference between HEK-293 and HEK-293S cells was determined using Student's t-test where *, $p < 0.05$, **, $p < 0.01$. (C) Correlation of log agonist potencies (\pm SEM) for CGRP, AM and AM2 at RAMP-CLR combinations expressed in HEK-293S (Table 4) cells and either HEK-293 cells with (red symbol) or without (blue symbol) pre-treatment with PTX (Table 3) was analyzed by a scatter plot and Pearson's correlation coefficients (r) were calculated. A significant correlation was observed only between HEK-293S cells and HEK-293 cells pre-treated with PTX.

Figure 7. Functional coupling of CLR co-transformed with all three RAMPs to the $G\alpha_q$ chimera. Dose response curves to CGRP, AM and AM2 were constructed in yeast strains containing the GPA1/ $G\alpha_q$ chimera and expressing CLR with (A), RAMP1 ($n = 7$) (B), RAMP2 ($n = 6$) and (C), RAMP3 ($n = 7$). Reporter gene activity was determined following 24 h stimulation. All data are expressed as percentage of the maximum response observed in a yeast strain MMY11 and are means \pm SEM of n individual data sets. (D) Bar chart showing the efficacy of each ligand for each RAMP-CLR combination at the $G\alpha_q$ chimera determined via application of the operational model of receptor agonism ((34); Table 1). Data were determined as statistically different from the cognate ligand for each receptor (*, $p < 0.05$, **, $p < 0.01$, ***, $p < 0.001$) using a one-way ANOVA with Bonferroni's post-test. (E) Signaling bias plots were calculated as $\Delta\Delta(\tau/Ka)$ values on a logarithmic scale for each ligand and for each chimera G protein for the three individual RAMP-CLR complexes. Determination of values requires normalization to a reference ligand (CGRP for RAMP1-CLR and AM for CLR with RAMP2 or RAMP3) and a reference pathway (in all cases GPA1/ $G\alpha_s$).

Figure 8. CLR in combination with each RAMP generates receptors that mobilize $i(Ca^{2+})$ release when expressed in HEK-293 cells. $i(Ca^{2+})$ mobilization was determined from HEK-293 cells transiently transfected

with CLR and (A), RAMP1 ($n = 5$) (B), RAMP2 ($n = 5$) and (C), RAMP3 ($n = 5$). Cells were stimulated for 2 min with CGRP, AM and AM2 and data are expressed as percentage of the maximal $i(\text{Ca}^{2+})$ release as determined using 10 μM ionomycin. To determine the contribution made by different G proteins to the $i(\text{Ca}^{2+})$ response, cells were pre-incubated with either PTX (to inhibit $\text{G}\alpha_i$) or YM-254890 (a selective $\text{G}\alpha_q$ inhibitor). All values are means \pm SEM of n individual data sets.

Figure 9. Quantification of biased agonism at the three RAMP-CLR complexes. (A) Normalized transduction coefficients, $\Delta\log(\tau/\text{Ka})$, for cAMP accumulation and $i(\text{Ca}^{2+})$ mobilization obtained for the three RAMP-CLR complexes upon stimulated with CGRP, AM or AM2 in untreated HEK-293 cells, HEK-293 cells treated with PTX and HEK-293S cells. (B) Relative bias factors, $\Delta\Delta(\tau/\text{Ka})$, for cAMP accumulation and $i(\text{Ca}^{2+})$ mobilization for the three individual RAMP-CLR complexes upon stimulated with CGRP, AM or AM2 in untreated HEK-293 cells, HEK-293 cells treated with PTX and HEK-293S cells. Determination of values requires normalization to a reference ligand (CGRP for RAMP1-CLR and AM for CLR with RAMP2 or RAMP3) and a reference pathway (in all cases cAMP accumulation).

Figure 10. Class B GPCR:RAMP Heterodimeric Models and Molecular Dynamics Simulations. Molecular models and dynamic simulation suggest that the C-terminal tail of RAMP1/2 (olive/yellow) when in complex with either (A) GCGR (blue) or (B) CLR (teal) makes a direct interaction with the bound C-terminal of $\text{G}\alpha_s$ (green) and or helix 8. The glucagon peptide agonist is shown in magenta and CGRP is shown in purple. (C) The RAMP2 C-terminus approaches toward $\text{G}\alpha_s$ (red arrow) during a molecular dynamics simulations of an active GCGR-RAMP2-glucagon complex. RAMP2 is yellow, $\text{G}\alpha_s$ is green, and the GCGR is coloured according to time progression, from red (0 ns) to blue (500 ns).

Figure 11. The peptide agonist, the GPCR TM7 and the RAMP TM helix move as a collective unit during molecular dynamics simulations. (A) Schematic diagram of the distances between the members of the collective unit and TM2. Top arrow bars indicate the following distances in order: RAMP2-TM2 (green), TM7-TM2 (cyan), peptide-TM2 (orange). Bottom arrow bars indicate the distances within the members of the collective unit in order: RAMP2-peptide (purple), RAMP-TM7 (black), TM7-peptide (red). (B) Distances from each of the collective unit components (RAMP TM, TM7 and glucagon agonist) to TM2 (order as above); these distances decrease in a similar manner, reflecting their concerted movement. (C) Distances between each of the collective unit components (RAMP, TM7 and glucagon agonist) (order as above); these distances are relatively constant, reflecting their movement as a collective unit.

Figure 12. Agonist potency ratios for CGRP, AM and AM2 at the CLR in combination with each RAMP. Log potency ratios (as measured by accumulation of intracellular cAMP) are defined as $\text{Log}[\text{EC}_{50} \text{ AM2} \div \text{EC}_{50} \text{ Agonist}]$. Data taken from Hong *et al.* (1) supplemented with references (43, 44). HEK-293 and HEK-293S cell data from the current study are shown in red and blue, yeast $\text{G}\alpha_s$ coupling is shown in green.

Figure 13. A working model of biased-agonism at the different RAMP-CLR complexes. The individual RAMP-CLR complexes can bind the agonists CGRP (red), AM (Green) and AM2 (Blue) to activate different downstream chimeric GPA1/ $\text{G}\alpha$ subunits (in yeast) or promote increases in intracellular cAMP and/or mobilize release of $i(\text{Ca}^{2+})$ (in HEK-293/HEK-293S cells). The thickness of lines indicates the bias that each agonist displays for either the chimeric G protein or the specific downstream signaling cascade. The yeast system enables comparison of different individual G proteins ($\text{G}\alpha_s$, $\text{G}\alpha_{i/2}$ and $\text{G}\alpha_q$) while mammalian cells investigate cAMP accumulation (\pm PTX) and elevation of $i(\text{Ca}^{2+})$.

Figure 1

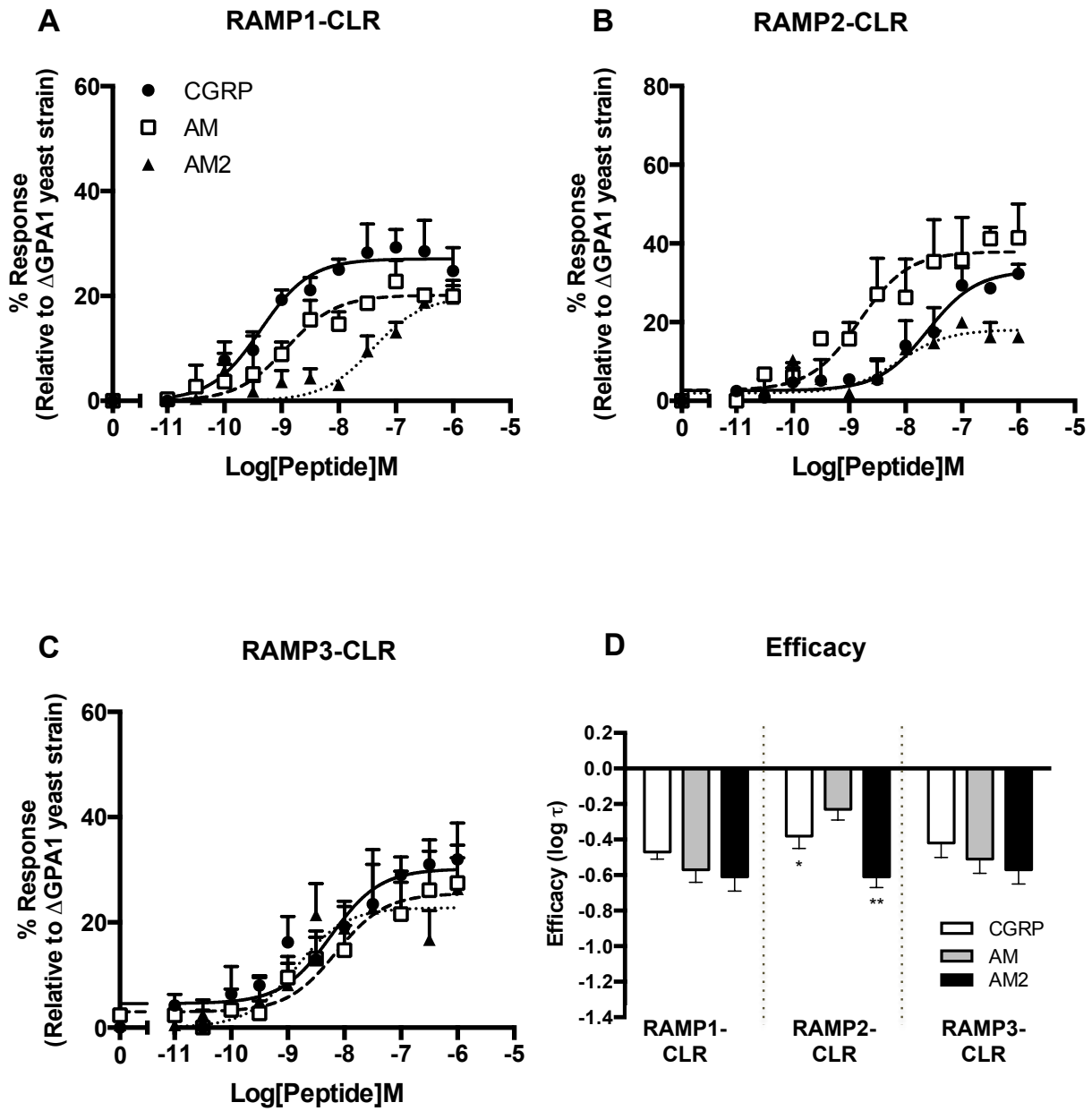


Figure 2

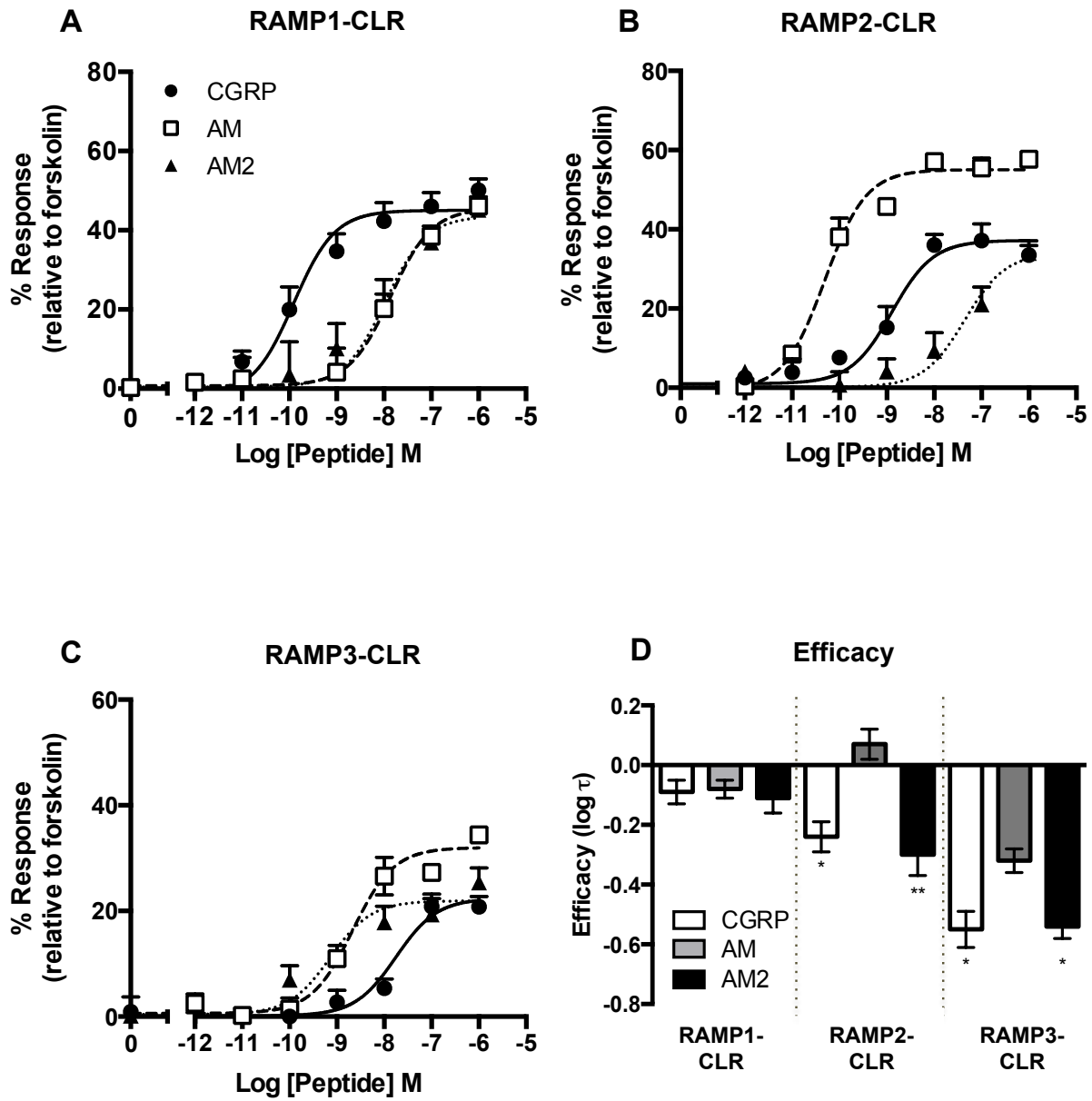


Figure 3

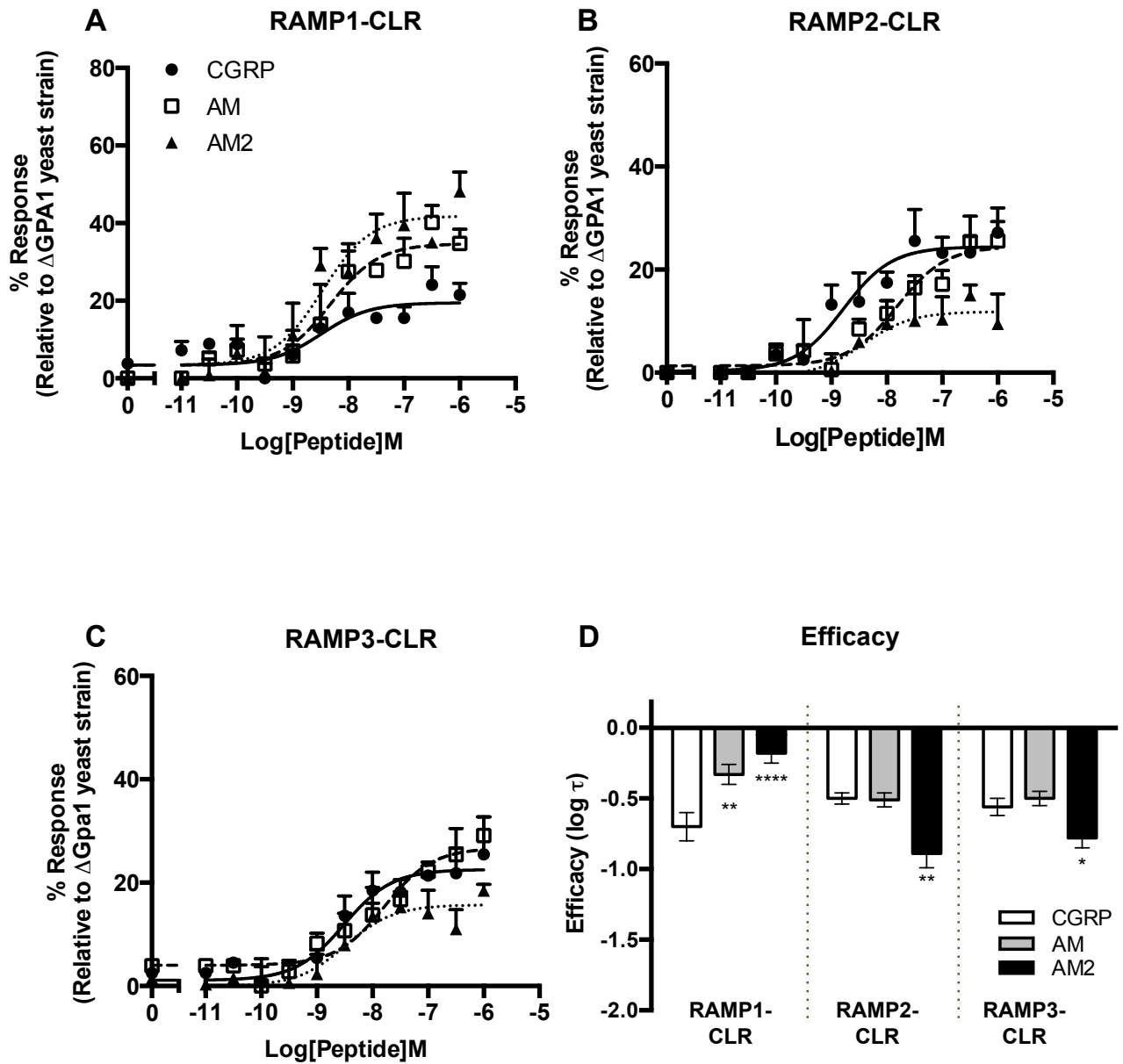


Figure 4

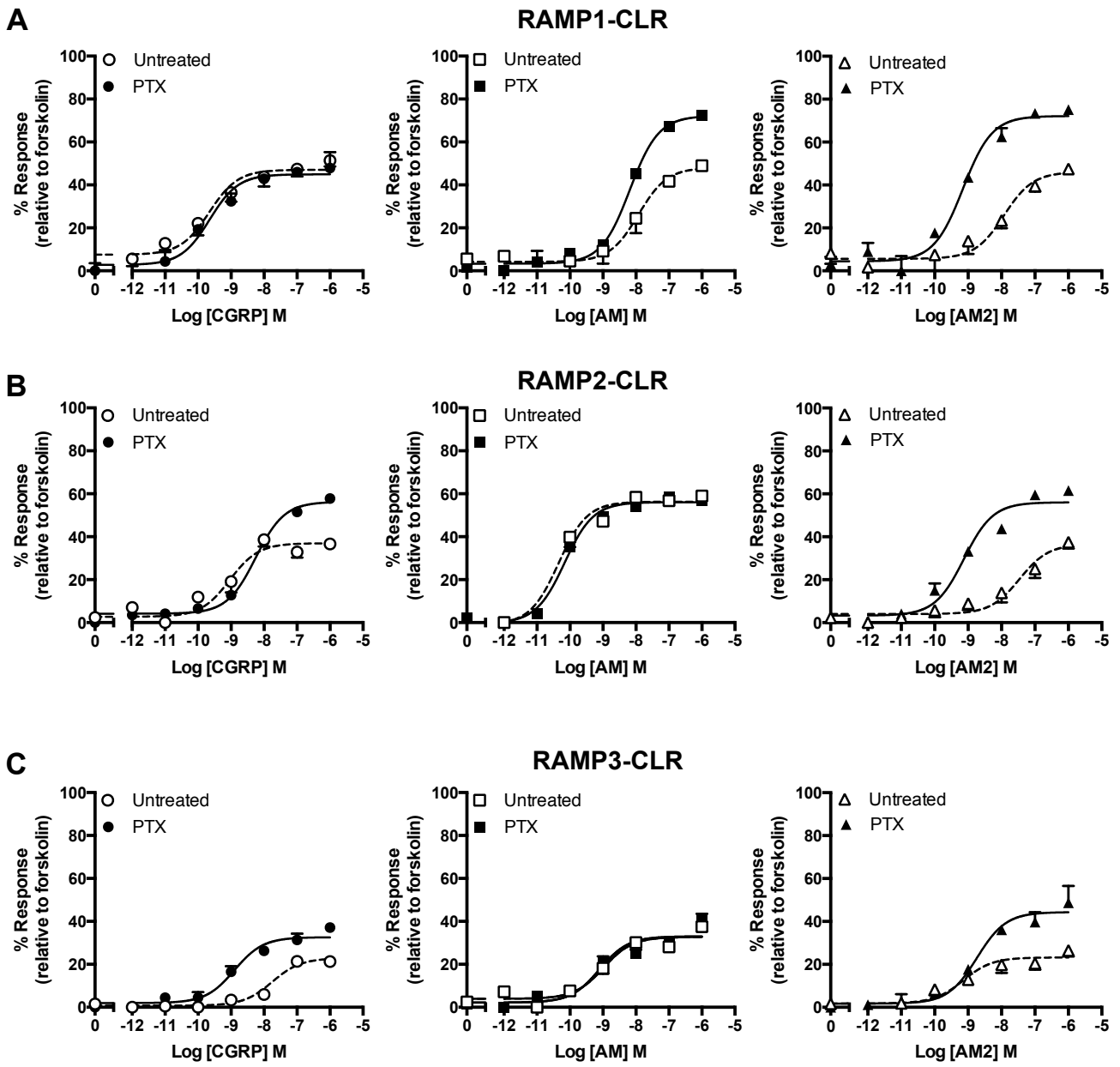


Figure 5

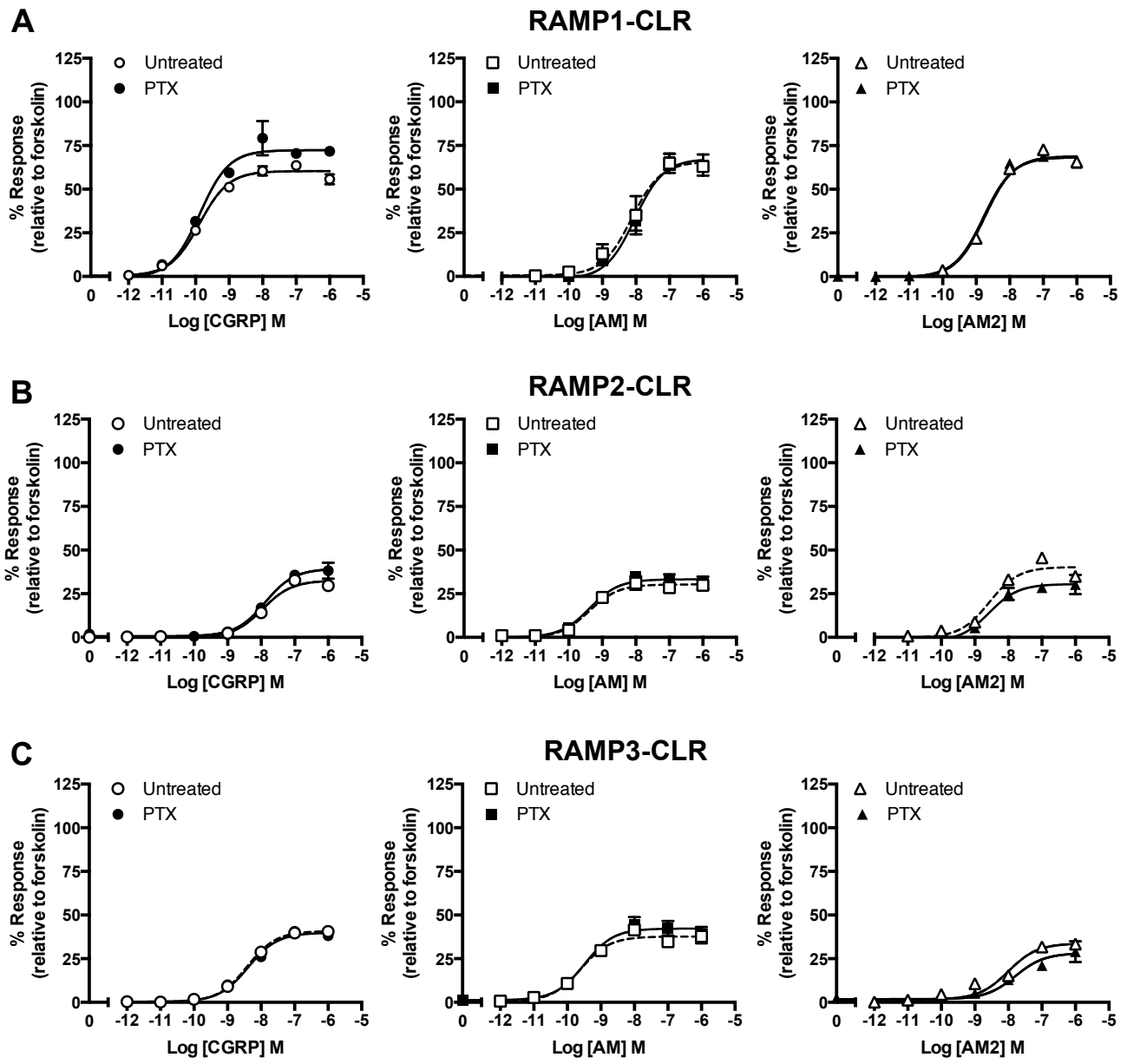


Figure 6

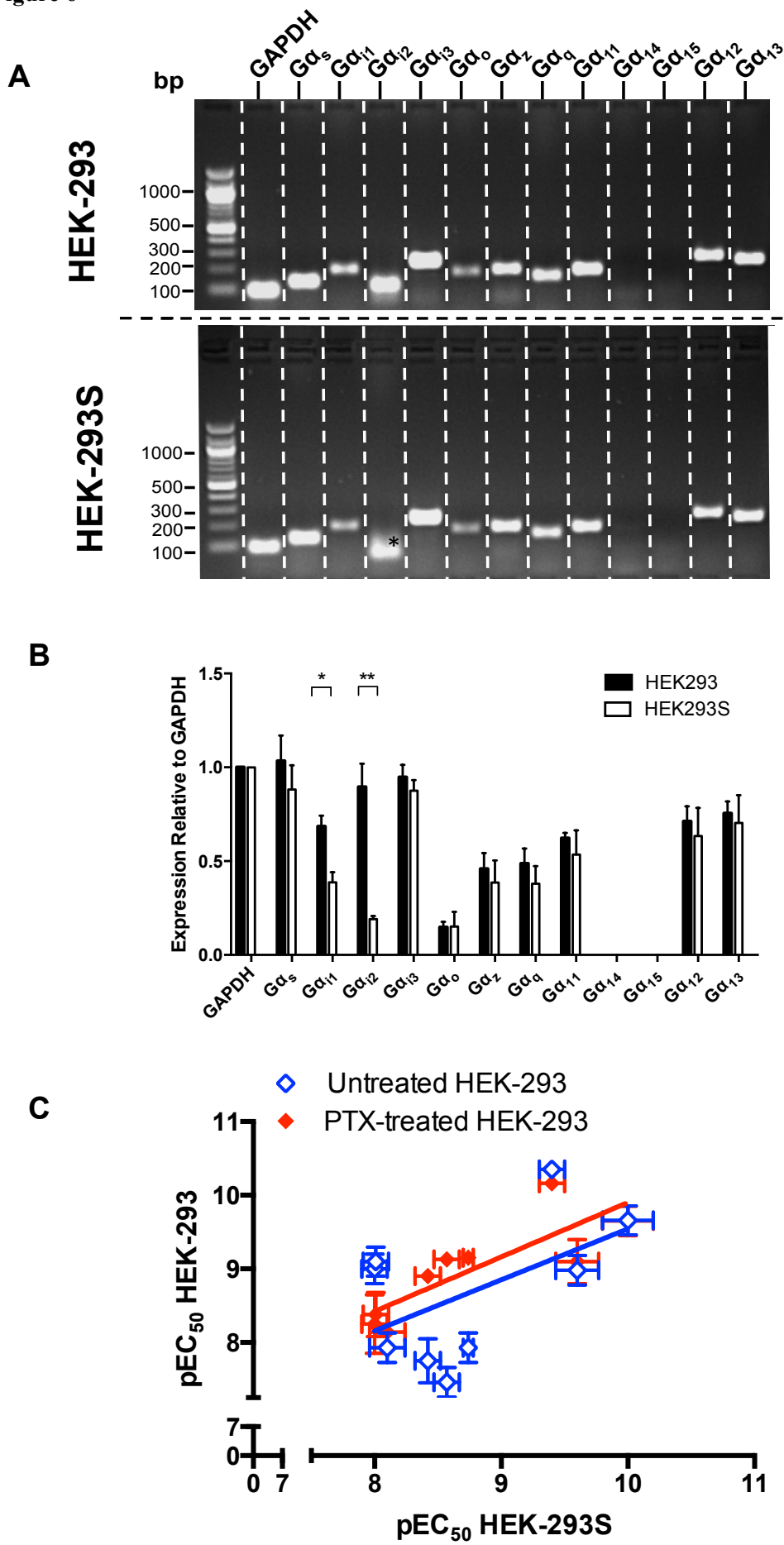


Figure 7

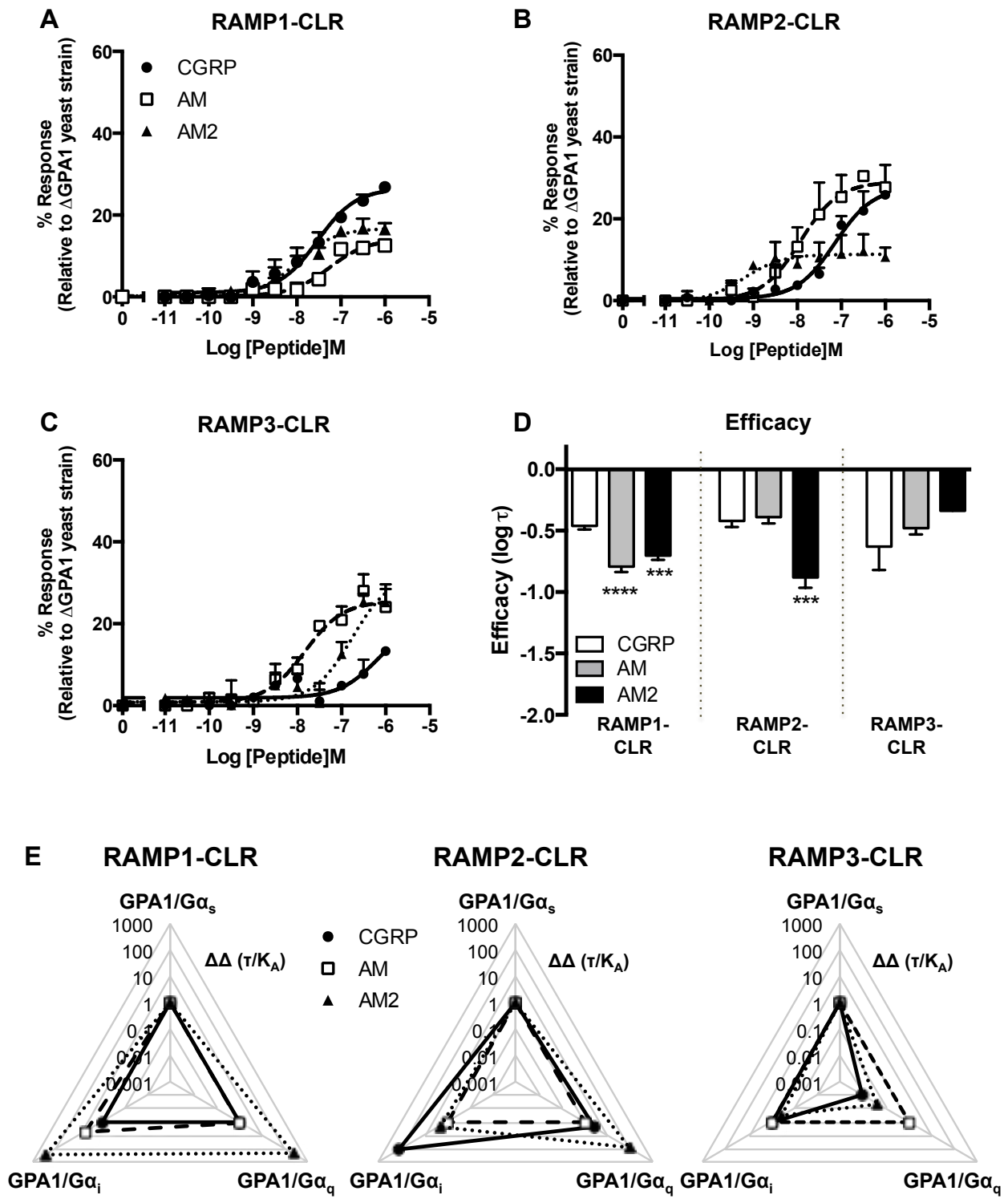


Figure 8

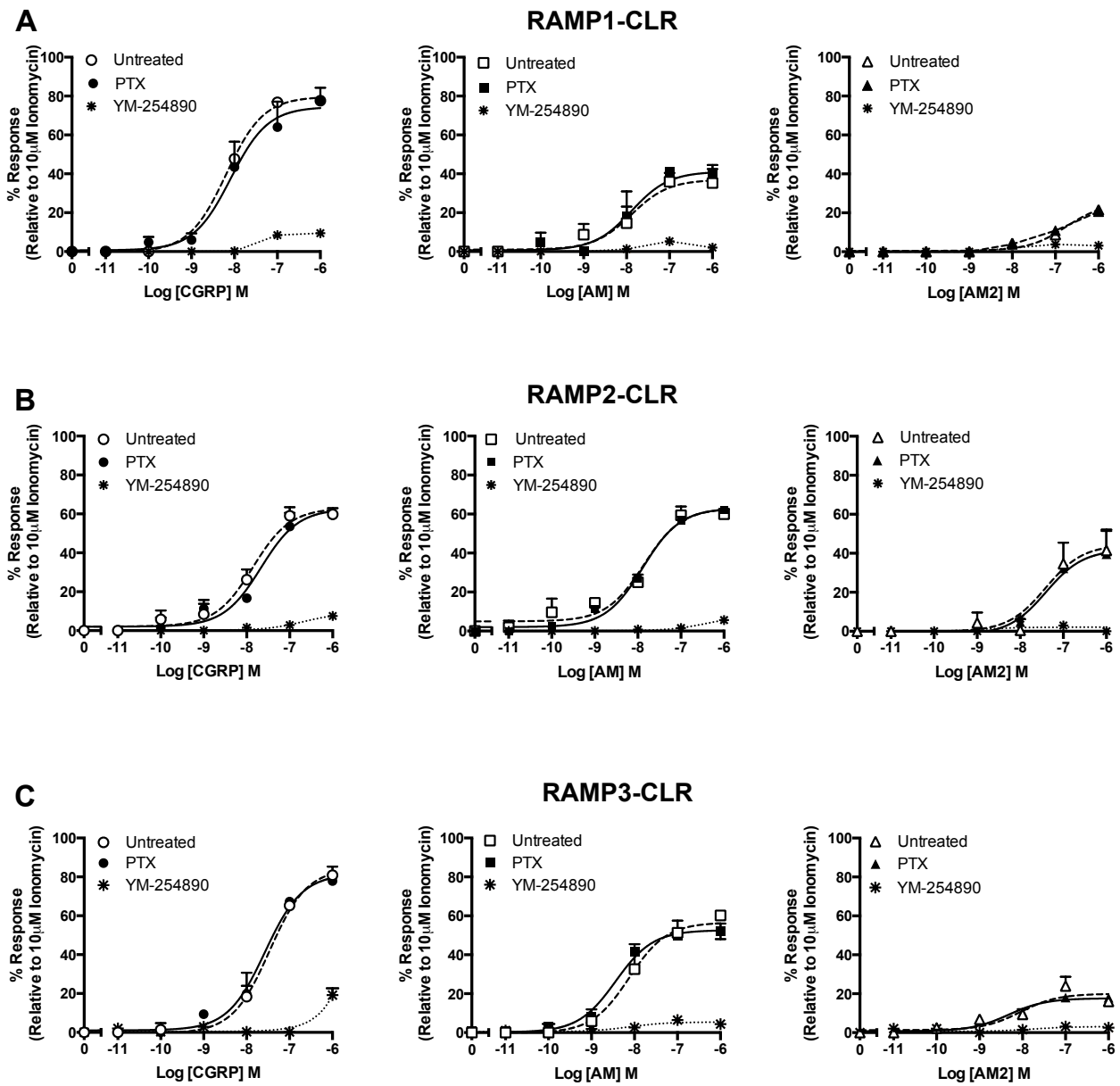


Figure 9

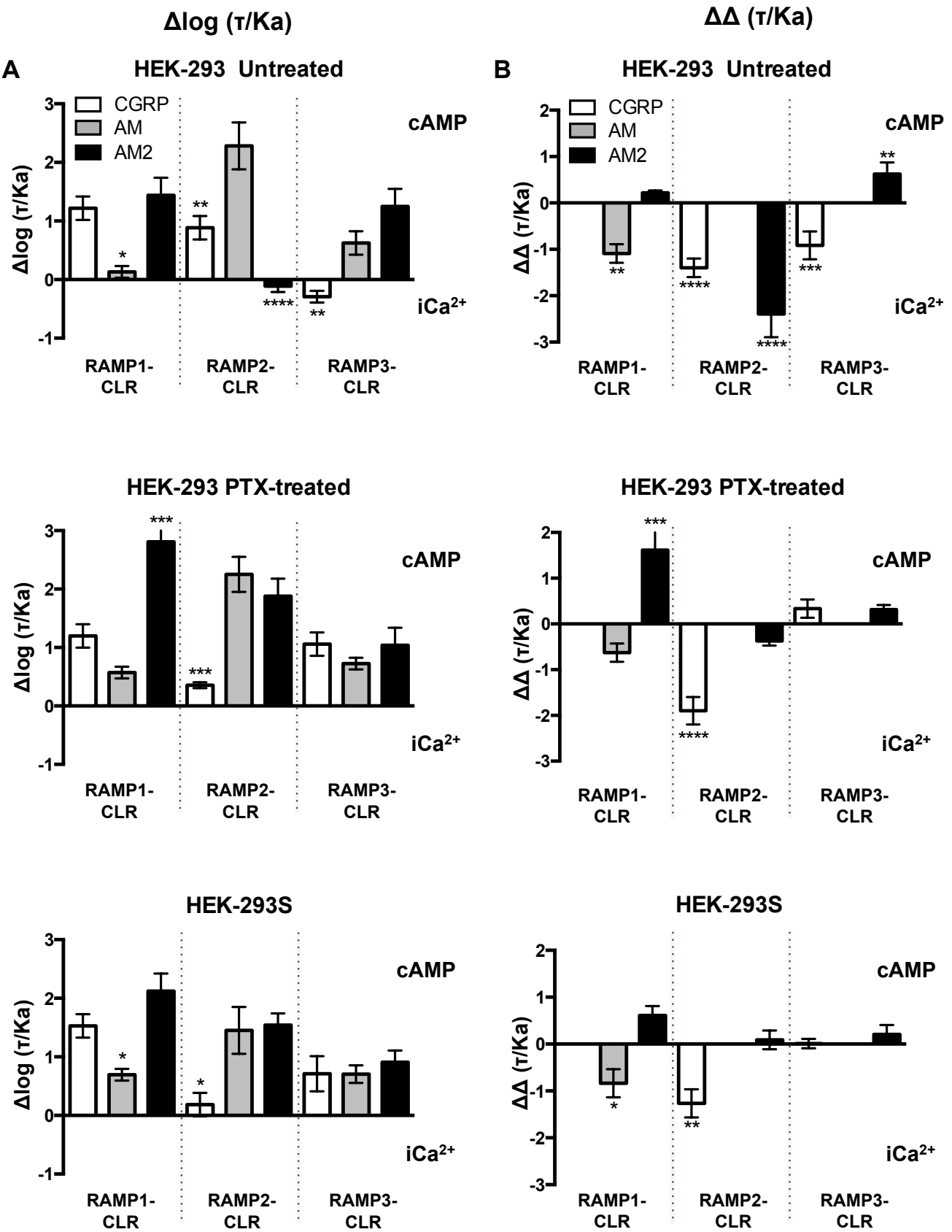


Figure 10

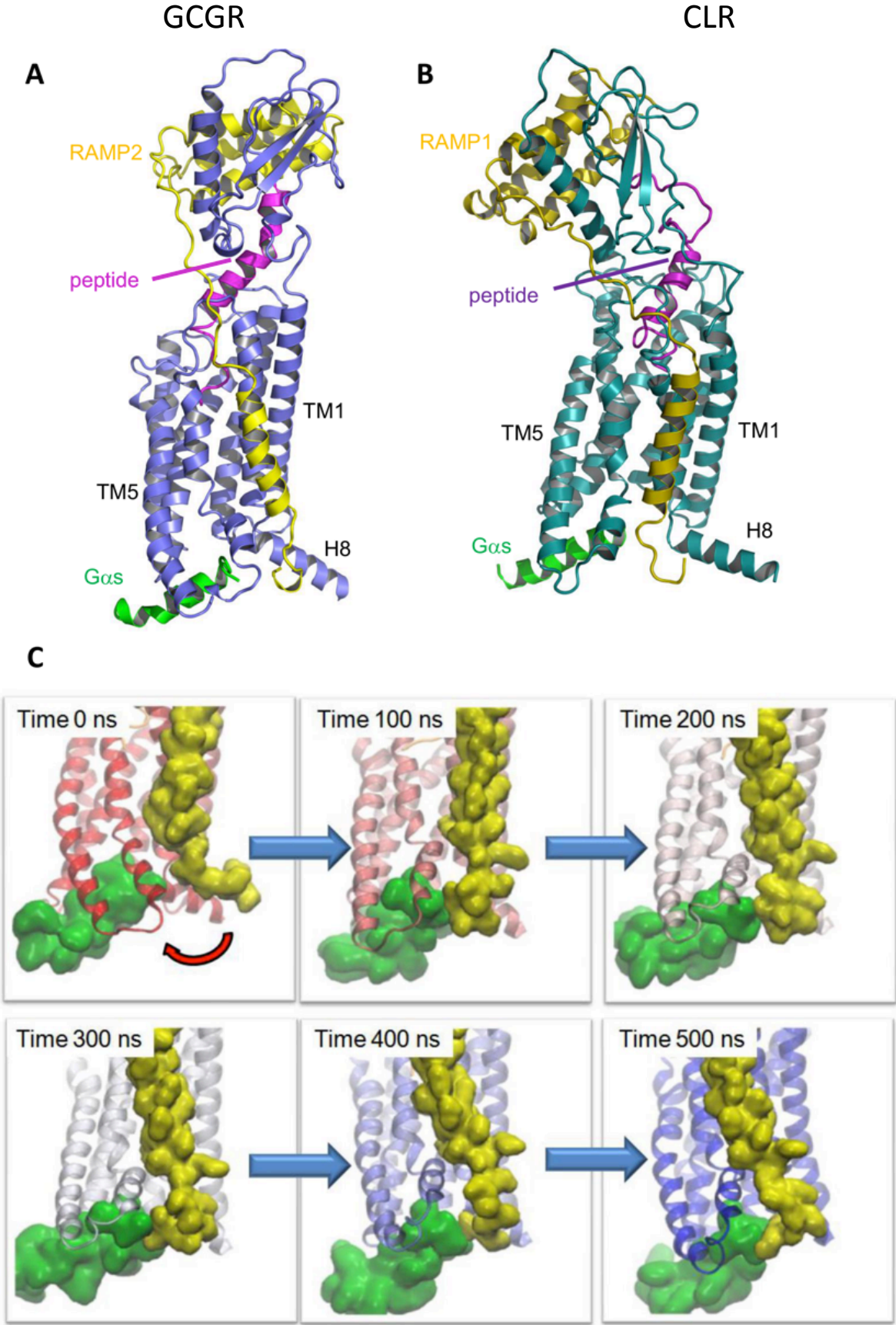


Figure 11

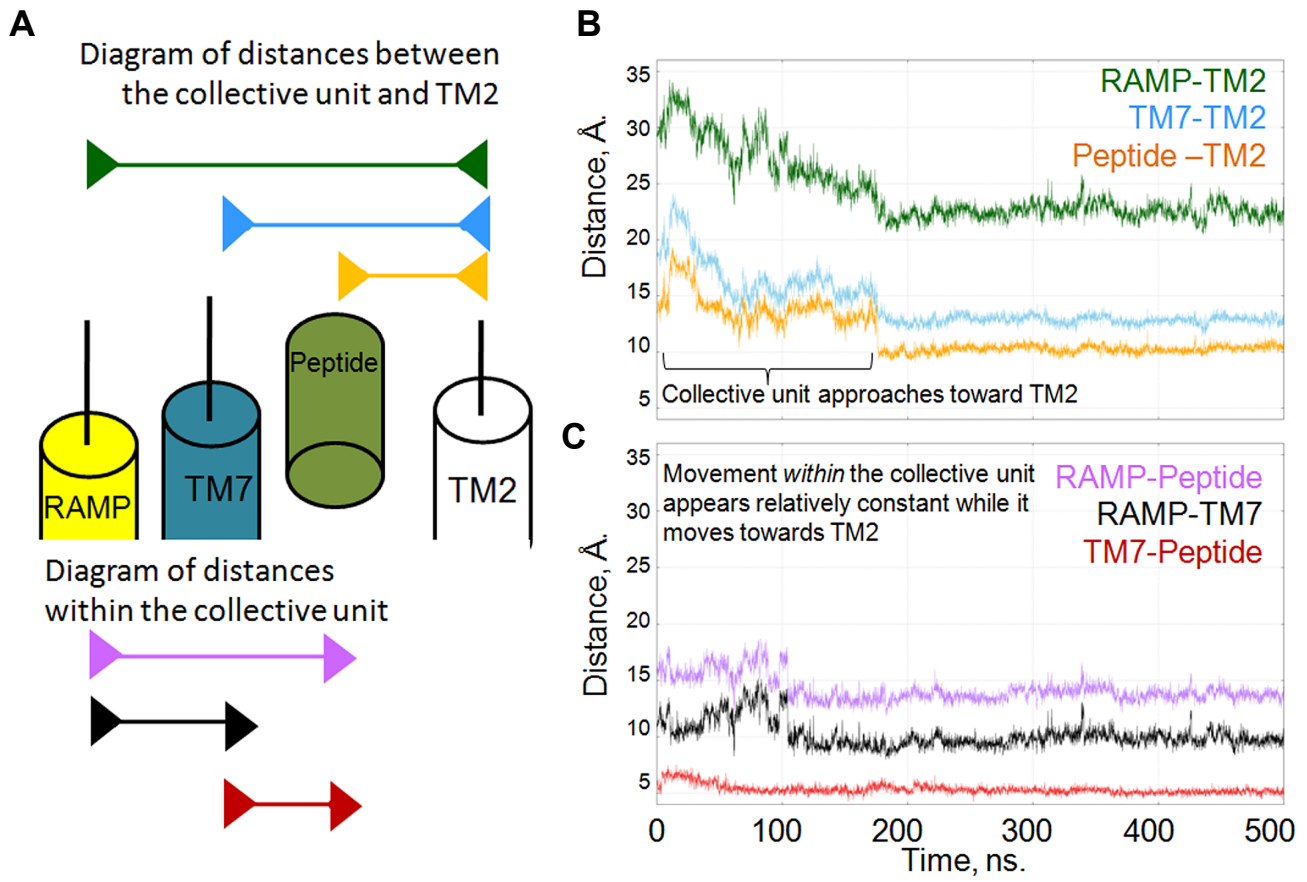


Figure 12

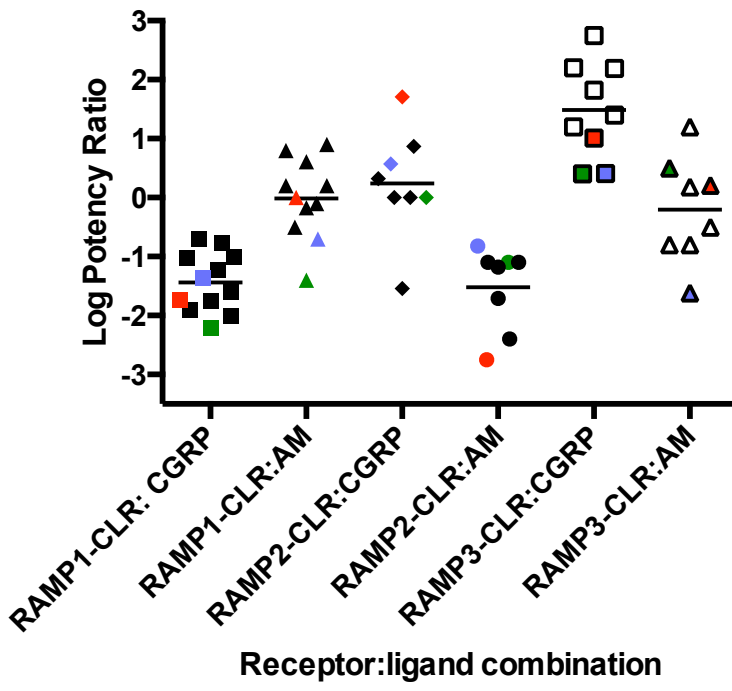


Figure 13

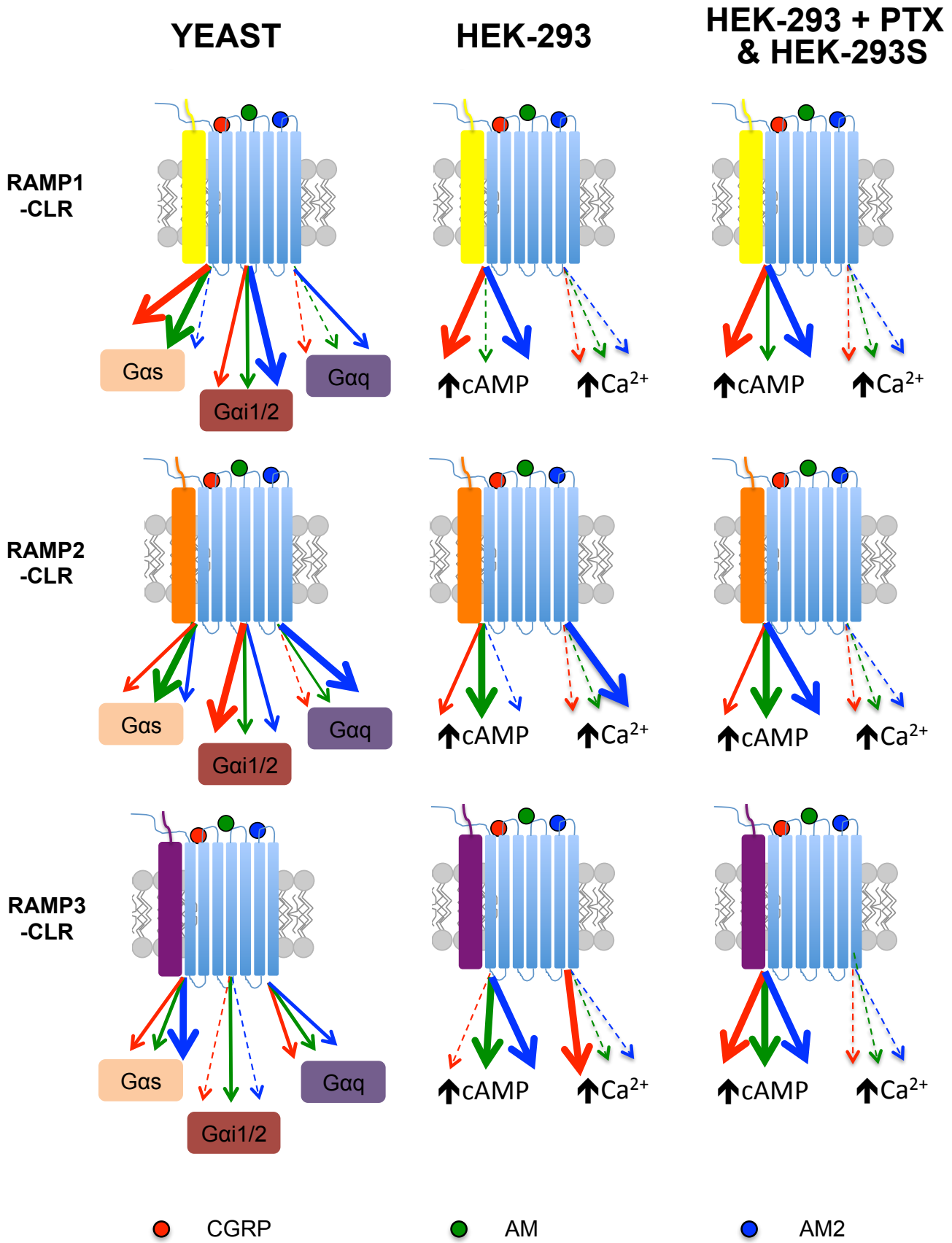


Table 1: Summary table of pharmacological parameters for various ligands upon expression of the CLR with each RAMP in yeast strains containing the GPA1/G α_s , GPA1/G α_i or the GPA1/G α_q chimera.

	GPA1/G α_s								
	RAMP1-CLR			RAMP2-CLR			RAMP3-CLR		
	CGRP	AM	AM2	CGRP	AM	AM2	CGRP	AM	AM2
pEC₅₀^a	9.35±0.2	8.80±0.4**	7.22±0.3***	7.60±0.3*	8.82±0.3	8.05±0.3	8.24±0.2	8.15±0.4	8.85±0.3
E_{max}^b	27.10±1.6	20.39±2.8	20.65±1.1	30.34±4.1	37.46±3.5	19.90±2.5***	30.17±2.7	25.51±3.6	22.80±2.3
pKa^c	9.22±0.2	8.81±0.3***	7.31±0.3***	7.70±0.3*	8.77±0.3	8.10±0.3	8.30±0.3	8.10±0.3	8.61±0.4
logτ^d	-0.43±0.04	-0.59±0.07	-0.61±0.08	-0.38±0.08*	-0.23±0.06	-0.61±0.06**	-0.42±0.08	-0.51±0.08	-0.57±0.08
n	6	6	6	7	7	7	8	8	8
	GPA1/G α_i								
	RAMP1-CLR			RAMP2-CLR			RAMP3-CLR		
	CGRP	AM	AM2	CGRP	AM	AM2	CGRP	AM	AM2
pEC₅₀^a	8.26±0.5	8.38±0.3	8.57±0.2	8.89±0.2	7.91±0.2**	8.42±0.5	8.52±0.2	7.89±0.8	8.49±0.2
E_{max}^b	19.80±3.0	34.20±3.7***	41.5±3.3****	24.43±1.7	24.49±2.0	15.71±2.5*	22.60±1.8	26.71±1.8	15.71±2.1*
pKa^c	8.40±0.5	8.20±0.3	8.24±0.2	8.64±0.2	7.75±0.2	8.30±0.5	8.37±0.2	8.00±0.2	8.30±0.3
logτ^d	-0.70±0.1	-0.33±0.07**	-0.18±0.1***	-0.50±0.04	-0.51±0.05	-0.89±0.1**	-0.56±0.06	-0.50±0.05	-0.78±0.07*
n	6	6	6	6	6	6	7	7	7
	GPA1/G α_q								
	RAMP1-CLR			RAMP2-CLR			RAMP3-CLR		
	CGRP	AM	AM2	CGRP	AM	AM2	CGRP	AM	AM2
pEC₅₀^a	7.53±0.1	7.26±0.2	7.99±0.2	7.14±0.2	7.93±0.2	9.22±0.4*	6.19±0.5*	7.83±0.2	6.76±0.25
E_{max}^b	26.50±1.2	14.08±1.2****	16.73±1.1****	27.74±2.3	29.03±2.6	11.33±1.3****	20.7±4.2	25.56±2.0	32.11±3.7
pKa^c	7.40±0.1	7.19±0.2	7.91±0.03	7.01±0.2	7.78±0.2	9.16±0.4*	6.10±0.6*	7.71±0.2	6.60±0.3
logτ^d	-0.46±0.03	-0.79±0.04***	-0.70±0.04***	-0.42±0.05	-0.39±0.05	-0.88±0.08***	-0.63±0.2	-0.48±0.05	-0.34±0.1
n	7	7	7	6	6	6	6	6	6

Data are the mean \pm SEM of n individual data sets (in parentheses).

^a The negative logarithm of the agonist concentration required to produce a half-maximal response.

^b The maximal response to the ligand expressed as a percentage of that obtained from a yeast strain (MMY11) lacking GPA1.

^c The negative logarithm of the equilibrium disassociation constant for each ligand generated through use of the operational model of agonism (34).

^d τ is the coupling efficiency parameter of each ligand.

Statistical significance compared to the cognate ligand (*, $p < 0.05$, **, $p < 0.01$, ***, $p < 0.001$, ****, $p < 0.0001$) for each receptor heterodimer (CGRP for RAMP1 + CLR; AM for CLR with either RAMP2 or RAMP3) was determined by one-way ANOVA with Dunnett's post-test.

Table 2: Potency (pEC_{50}), affinity (pK_a) and coupling efficacy ($\log \tau$) values for cAMP production at the CLR co-expressed with each RAMP and stimulated with various agonists measured in HEK-293 cells.

	RAMP1-CLR			RAMP2-CLR			RAMP3-CLR		
	CGRP	AM	AM2	CGRP	AM	AM2	CGRP	AM	AM2
pEC_{50}^a	9.81±0.20	7.92±0.19**	7.93±0.24**	8.97±0.24***	10.35±0.13	7.48±0.23***	7.75±0.3**	8.86±0.14	9.14±0.22
E_{max}^b	45.0±2.2	45.2±3.7	43.6±4.2	37.2±2.4**	55.0±1.7	34.1±4.0**	22.3±2.1**	32.1±1.6	21.9±1.7**
pK_a^c	9.60±0.18	7.64±0.28**	7.76±0.20**	8.71±0.2	9.95±0.23	7.16±0.24	7.64±0.26	8.50±0.19	9.00±0.18*
$\log \tau^d$	-0.08±0.04	-0.08±0.09	-0.11±0.06	-0.23±0.05*	0.09±0.05	-0.29±0.07**	-0.54±0.06*	-0.33±0.04	-0.56±0.04*
n	11	11	11	8	8	8	9	9	9

Data are the mean \pm SEM of n individual data sets.

^a The negative logarithm of the agonist concentration required to produce a half-maximal response.

^b The maximal response to the ligand expressed as a percentage of the maximal cAMP production as determined using 100 μ M forskolin stimulation.

^c The negative logarithm of the equilibrium disassociation constant for each ligand generated through use of the operational model of agonism (34).

^d τ is the coupling efficiency parameter of each ligand.

Statistical significance compared to the cognate ligand (*, $p < 0.05$, **, $p < 0.01$, ***, $p < 0.001$, ****, $p < 0.0001$) for each receptor heterodimer (CGRP for RAMP1-CLR; AM for CLR with either RAMP2 or RAMP3) was determined by one-way ANOVA with Dunnett's post-test.

Table 3: Potency (pEC_{50}), affinity (pKa) and coupling efficacy ($\log \tau$) values for cAMP production at the CLR co-expressed with each RAMP, stimulated with various agonists measured in HEK-293 cells in the presence and absence of pertussis toxin.

RAMP1	Untreated					Treated				
	pEC_{50}^a	E_{max}^b	pKa^c	$\log\tau^d$	n	pEC_{50}^a	E_{max}^b	pKa^c	$\log\tau^d$	n
CGRP	9.66±0.2	47.07±2.2	9.43±0.2	-0.11±0.04	9	9.65±0.2	44.95±2.2	9.33±0.3	-0.11±0.07	6
AM	7.93±0.2	48.06±2.5	7.67±0.2	-0.09±0.05	9	8.14±0.07	72.17±1.7***	7.66±0.2	0.36±0.1**	6
AM2	7.93±0.2	46.10±4.1	7.70±0.2	-0.11±0.07	9	9.15±0.1*	72.15±2.4***	8.56±0.3	0.40±0.1**	6
RAMP2	Untreated					Treated				
	pEC_{50}^a	E_{max}^b	pKa^c	$\log\tau^d$	n	pEC_{50}^a	E_{max}^b	pKa^c	$\log\tau^d$	n
CGRP	9.00±0.2	36.97±2.4	8.82±0.2	-0.27±0.05	9	8.25±0.4	56.27±1.4***	7.92±0.2*	0.1±0.06**	6
AM	10.35±0.1	56.33±1.6	10.00±0.1	0.07±0.02	9	10.16±0.07	56.07±1.1	9.83±0.2	0.07±0.02	6
AM2	7.46±0.2	36.61±3.5	7.24±0.2	-0.29±0.07	9	9.13±0.1**	56.05±2.2***	8.84±0.2**	0.1±0.06*	6
RAMP3	Untreated					Treated				
	pEC_{50}^a	E_{max}^b	pKa^c	$\log\tau^d$	n	pEC_{50}^a	E_{max}^b	pKa^c	$\log\tau^d$	n
CGRP	7.75±0.3	22.38±2.6	7.64±0.3	-0.54±0.07	8	8.90±0.1*	32.61±1.5*	8.74±0.2*	-0.29±0.06	7
AM	8.98±0.2	32.00±1.5	8.83±0.1	-0.33±0.03	8	9.10±0.2	35.95±2.2	8.94±0.2	-0.34±0.05	7
AM2	9.10±0.2	21.92±1.7	9.08±0.2	-0.51±0.06	8	8.74±0.2	44.35±2.7****	8.43±0.1*	-0.07±0.07***	7

Data are the mean ± SEM of n individual data sets.

^a The negative logarithm of the agonist concentration required to produce a half-maximal response.

^b The maximal response to the ligand expressed as a percentage of the maximal cAMP production as determined using 100 μ M forskolin stimulation in the presence of pertussis toxin treatment.

^c The negative logarithm of the equilibrium disassociation constant for each ligand generated through use of the operational model of agonism (34).

^d τ is the coupling efficiency parameter of each ligand.

Statistically different between PTX-treated and untreated was determined using Student's t-test (*, $p < 0.05$, **, $p < 0.01$, ***, $p < 0.001$, ****, $p < 0.0001$).

Table 4: Potency (pEC_{50}) and maximal response (E_{max}), for cAMP production at the CLR co-expressed with each RAMP, stimulated with various agonists measured in HEK-293S cells in the presence or absence of pertussis toxin.

RAMP1	Untreated			Treated		
	pEC_{50}^a	E_{max}^b	n	pEC_{50}^a	E_{max}^b	n
CGRP	9.88±0.1	59.98±1.1	5	9.87±0.1	72.92±2.3	5
AM	8.13±0.1	60.00±3.1	5	8.03±0.1	61.26±2.6	5
AM2	8.74±0.1	68.94±1.2	5	8.78±0.1	68.30±1.6	5
RAMP2	Untreated			Treated		
	pEC_{50}^a	E_{max}^b	n	pEC_{50}^a	E_{max}^b	n
CGRP	8.00±0.1	32.56±1.0	5	7.88±0.1	39.32±1.7	5
AM	9.39±0.1	30.34±0.8	5	9.38±0.1	33.28±1.2	5
AM2	8.57±0.1	40.30±1.5	5	8.58±0.16	30.52±2.0	5
RAMP3	Untreated			Treated		
	pEC_{50}^a	E_{max}^b	n	pEC_{50}^a	E_{max}^b	n
CGRP	8.42±0.1	40.84±0.6	5	8.38±0.1	39.84±1.0	5
AM	9.63±0.1	39.09±1.2	5	9.49±0.2	42.26±1.6	5
AM2	8.01±0.1	33.75±1.5	5	7.79±0.2	28.21±2.4	5

Data are the mean \pm SEM of n individual data sets.

^a The negative logarithm of the agonist concentration required to produce a half-maximal response.

^b The maximal response to the ligand expressed as a percentage of the maximal cAMP production as determined using 100 μ M forskolin stimulation in the presence of PTX treatment.

No statistical difference was found between untreated and PTX-treated HEK-293S cells using Student's t-test.

Table 5: Potency (pEC₅₀), affinity (pKa) and coupling efficacy (log τ) values for i(Ca²⁺) mobilization at the CLR co-expressed with each RAMP, stimulated with various agonists measured in HEK-293 and HEK-293S cells.

RAMP1	HEK-293					HEK-293S				
	pEC ₅₀ ^a	E _{max} ^b	pKa ^c	log τ ^d	n	pEC ₅₀ ^a	E _{max} ^b	pKa ^c	log τ ^d	n
CGRP	8.19±0.1	79.68±0.7	7.50±0.1	0.60±0.05	5	8.06±0.1	67.64±2.0	7.57±0.1	0.32±0.04	5
AM	7.90±0.2	37.00±3.5 ^{****}	7.69±0.4	-0.24±0.10	5	7.63±0.2	38.18±3.8 ^{****}	7.42±0.2	-0.21±0.07 ^{****}	5
AM2	6.76±0.2 ^{***}	25.05±2.4 ^{****}	6.64±0.1 ^{**}	-0.48±0.06 ^{**}	5	6.94±0.1 ^{***}	33.28±1.7 ^{****}	6.76±0.1 ^{**}	-0.30±0.03 ^{****}	5
RAMP2	HEK-293					HEK-293S				
	pEC ₅₀ ^a	E _{max} ^b	pKa ^c	log τ ^d	n	pEC ₅₀ ^a	E _{max} ^b	pKa ^c	log τ ^d	n
CGRP	7.86±0.1	63.20±3.0	7.43±0.1	0.54±0.10	5	7.55±0.3	55.35±4.5	7.21±0.3	0.07±0.08	5
AM	7.86±0.1	63.00±1.8	7.45±0.2	0.19±0.06	5	7.68±0.2	52.26±4.5	7.39±0.2	0.03±0.10	5
AM2	7.41±0.4	44.41±7.1 [*]	7.15±0.4	-0.10±0.13 ^{**}	5	7.42±0.4	20.17±2.8 ^{****}	7.33±0.2	-0.65±0.13 ^{***}	5
RAMP3	HEK-293					HEK-293S				
	pEC ₅₀ ^a	E _{max} ^b	pKa ^c	log τ ^d	n	pEC ₅₀ ^a	E _{max} ^b	pKa ^c	log τ ^d	n
CGRP	7.47±0.2 [*]	84.39±8.5 [*]	6.66±0.4 [*]	0.74±0.26	5	7.51±0.2	65.3±4.7	7.07±0.2 ^{**}	0.24±0.10 [*]	5
AM	8.12±0.1	56.69±6.6	7.76±0.3	0.13±0.13	5	8.02±0.2	44.3±3.2	8.56±0.2	-0.11±0.06	5
AM2	8.05±0.3	19.99±2.4 [*]	7.95±0.3 [*]	-0.63±0.08 [*]	5	7.44±0.3	20.1±4.3	7.35±0.3 ^{**}	-0.62±0.07 ^{**}	5

Data are the mean ± SEM of *n* individual data sets.

^a The negative logarithm of the agonist concentration required to produce a half-maximal response.

^b The maximal response to the ligand expressed as a percentage of the maximal i(Ca²⁺) release as determined using 10 μ M ionomycin stimulation.

^c The negative logarithm of the equilibrium disassociation constant for each ligand generated through use of the operational model of agonism (34).

^d τ is the coupling efficiency parameter of each ligand.

Statistical significance compared to the cognate ligand (*, $p < 0.05$, **, $p < 0.01$, ***, $p < 0.001$, ****, $p < 0.0001$) for each receptor heterodimer (CGRP for RAMP1-CLR; AM for CLR with either RAMP2 or RAMP3) was determined by one-way ANOVA with Dunnett's post-test.

Supplementary Movie 1.

The RAMP2 C-terminus (yellow surface, right hand side) approaches toward $G\alpha_s$ (green surface, left hand side) during a molecular dynamics simulations of an active RAMP2-GCGR-glucagon- $G\alpha_s$ complex. The GCGR (ribbon representation) is coloured according to time progression, from red (0 ns) to blue (500 ns).

Supplementary Movie 2.

The RAMP1 C-terminus (yellow surface, right hand side) approaches toward $G\alpha_s$ (blue surface, left hand side) during a 500 ns molecular dynamics simulations of an active RAMP1-CLR-CGRP- $G\alpha_s$ complex. CLR (ribbon representation) is coloured green. Part of the RAMP C-terminus also contacts H8 of CLR.

Receptor activity modifying protein-directed G protein signaling specificity for the calcitonin gene-related peptide family of receptors

Cathryn Weston, Ian Winfield, Matthew Harris, Rose Hodgson, Archana Shah, Simon J Dowell, Juan Carlos Mobarec, David A Woodcock, Christopher A Reynolds, David R Poyner, Harriet A Watkins and Graham Ladds

J. Biol. Chem. published online August 26, 2016

Access the most updated version of this article at doi: [10.1074/jbc.M116.751362](https://doi.org/10.1074/jbc.M116.751362)

Alerts:

- [When this article is cited](#)
- [When a correction for this article is posted](#)

[Click here](#) to choose from all of JBC's e-mail alerts

Supplemental material:

<http://www.jbc.org/content/suppl/2016/08/26/M116.751362.DC1.html>

This article cites 0 references, 0 of which can be accessed free at

<http://www.jbc.org/content/early/2016/08/26/jbc.M116.751362.full.html#ref-list-1>